Air quality trends and regimes in South Korea inferred from 2015−2023 surface and satellite observations

Yujin J. Oak[1], Daniel J. Jacob[1,2], Drew C. Pendergrass[1], Ruijun Dang[1], Nadia K. Colombi[2], Heesung Chong[3], Seoyoung Lee[4,5], Su Keun Kuk[6], Jhoon Kim[7]

[1] School of Engineering and Applied Sciences, Harvard University, Cambridge, MA, USA
[2] Department of Earth and Planetary Sciences, Harvard University, Cambridge, MA, USA
[3] Harvard-Smithsonian Center for Astrophysics, Cambridge, MA, USA
[4] Goddard Earth Sciences Technology and Research (GESTAR) II, University of Maryland, Baltimore County, Baltimore, MD, USA
[5] Climate and Radiation Laboratory, NASA Goddard Space Flight Center, Greenbelt, MD, USA
[6] Samsung Advanced Institute of Technology, Samsung Electronics Co., Ltd., Suwon, South Korea
[7] Department of Atmospheric Sciences, Yonsei University, Seoul, South Korea
Correspondence to: Yujin J. Oak (yjoak@g.harvard.edu)

Abstract.

We analyze 2015−2023 trends in air quality in South Korea using surface (AirKorea network) and satellite measurements, including the new GEMS geostationary instrument. Primary air pollutants (CO, SO_2, NO_2) have decreased steadily at rates consistent with the national CAPSS emissions inventory. Volatile organic compounds (VOCs) show no significant trend. GEMS glyoxal (CHOCHO) identifies large industrial sources of VOCs while formaldehyde (HCHO) points to additional biogenic sources. Surface ozone (O_3) peaks in May−June and the maximum 8-hour daily average (MDA8) exceeds the 60 ppbv standard everywhere. The AirKorea average May−June 90th percentile MDA8 O_3 increased at 0.8 ppbv a^{-1}, which has been attributed to VOC-sensitive conditions. Satellite HCHO/NO_2 ratios indicate that the O_3 production regime over Korea is shifting from VOC- to NO_x-sensitive conditions as NO_x emissions decrease. The O_3 increase at AirKorea sites is because most of these sites are in the Seoul Metropolitan Area where vestiges of VOC-sensitive conditions persist; we find no such O_3 increases over the rest of Korea where conditions are NO_x-sensitive or in the transition regime. Fine particulate matter ($PM_{2.5}$) has been decreasing at 5% a^{-1} in both AirKorea and satellite observations but the nitrate (NO_3^-) component has not been decreasing. Satellite NH_3/NO_2 ratios show that $PM_{2.5}$ NO_3^- formation was NH_3-sensitive before 2019 but is now becoming NO_x-sensitive as NO_x emissions decrease. Our results indicate that further NO_x emission decreases in Korea will reap benefits for both O_3 and $PM_{2.5}$ NO_3^- as their production is now dominantly NO_x-sensitive.

1. Introduction

South Korea experienced rapid development over the past 30 years with an annual average GDP growth rate of 5% (S. Song and G. Lee, 2020). This has resulted in high emissions of carbon monoxide (CO), sulfur dioxide (SO_2), nitrogen oxides ($NO_x \equiv NO + NO_2$), nonmethane volatile organic compounds (NMVOCs), and primary fine particulate matter ($PM_{2.5}$, smaller than 2.5 μm diameter) (Y. Kim and G. Lee, 2018). Subsequent atmospheric chemistry produces surface ozone (O_3) and additional $PM_{2.5}$, which are the main pollutants of concern for air quality. 30,000 premature deaths per year are presently attributed to air pollution in South Korea (hereafter referred to as Korea) (Oak et al., 2023; J. Choi et al., 2024). National air quality standards were tightened in 2018 for O_3 (60 ppbv maximum 8-hour daily average or MDA8) and for $PM_{2.5}$ (15 μg m^{-3} annual, 35 μg m^{-3} 24-hour). None of the sites in the AirKorea governmental surface network meet the O_3 standard as of 2022, and only 4% meet the 24-hour $PM_{2.5}$ standard, despite governmental efforts to decrease emissions.

The need to decrease emissions responsible for air pollution has been recognized since the 1980s, prompting early control policies to regulate solid fuel use and outdoor combustion, and promote clean fuels. This effectively reduced SO_2, CO, and directly emitted (primary) PM (Y. Kim and G. Lee, 2018). More recent efforts by the Korean Ministry of Environment (MOE) have targeted NO_x emissions. However, O_3 pollution has been getting worse at a rate of 1.0–1.5 ppbv a^{-1} over 2000–2021 (S. W. Kim et al., 2023). $PM_{2.5}$ has decreased though unevenly (J. Jeong et al., 2022; H. M. Lee et al., 2024; Pendergrass et al., 2022; 2024), with an increasing contribution from secondary components produced chemically in the atmosphere including secondary organic aerosol (SOA) and particulate nitrate (NO_3^-) (H. M. Lee et al., 2024).

Synoptic meteorology and transport from China also contribute to seasonal and long-term variations of pollutants over Korea. Photochemical O_3 production is largest during the summer months, but O_3 peaks in May–June due to the summer monsoon in July–August (H. M. Lee and R. Park, 2022). Wildfires, stratospheric intrusions, and transport from China also contribute to high O_3 levels during May–June (H. M. Lee and R. Park, 2022). $PM_{2.5}$ is highest during the colder months (October–March), due to increased energy consumption and stagnant conditions over the Korean peninsula (J. Jeong et al., 2024), but here again transport from China also makes an important contribution (D. Park et al., 2021). $PM_{2.5}$ pollution in China has decreased considerably over the past decade in response to emission controls (Zhai et al., 2019) and this has decreased its influence on Korea (Bae et al., 2021). On the other hand, O_3 pollution in China has gotten worse (K. Li et al., 2021).

Formation of O_3 and secondary $PM_{2.5}$ depends on complex chemistry involving NO_x and NMVOCs that would respond nonlinearly to emission controls. $PM_{2.5}$ NO_3^- formation further depends on ammonia (NH_3) emissions, which are mainly from agriculture and have not been decreasing. The dependences of O_3 and $PM_{2.5}$ concentrations on precursor emissions define chemical regimes that are important to understand for emission control strategies. They can be studied with 3-D chemical transport models (CTMs) that couple emissions, chemistry, and transport (R. Park et al., 2021). The formaldehyde (HCHO) to NO_2 ratio measured from satellite can diagnose O_3 sensitivity to VOCs versus NO_x emissions (Duncan et al., 2010; Martin et al., 2004), and the NH_3 to NO_2 ratio can diagnose NO_3^- sensitivity to NH_3 versus NO_x emissions (Dang et al., 2023; 2024).

Satellites offer a growing resource for monitoring air pollutants, trends, and regimes over Korea. Low-Earth orbit (LEO) instruments observe at specific times of day. Important instruments include MOPITT (Edwards et al., 2004) and TROPOMI (Veefkind et al., 2012) for CO, OMI (Levelt et al., 2006) and TROPOMI for SO_2, NO_2, HCHO, and glyoxal (CHOCHO), and IASI (Van Damme et al., 2014) for NH_3. Geostationary instruments over East Asia including GOCI and GOCI-II provide hourly observations of aerosol optical depth (AOD) (M. Choi et al., 2018; S. Lee et al., 2023). The Geostationary Environment Monitoring Spectrometer (GEMS), launched in February 2020, provides the first hourly observations of gases by solar backscatter including SO_2, NO_2, HCHO, and CHOCHO (J. Kim et al., 2020).

Here we analyze recent 2015−2023 trends in air quality in Korea by exploiting both satellite and surface observations. We interpret the trends in terms of the major drivers and evaluate consistency with annual bottom-up emission estimates from the Clean Air Policy Support System (CAPSS) of the MOE (S. Choi et al., 2022). We start from 2015 when $PM_{2.5}$ observations from the AirKorea network became available, with subsequent milestones including the May−June 2016 Korea-United States Air Quality (KORUS-AQ) field campaign (Crawford et al., 2021) and satellite observations from TROPOMI (starting in May 2018) and GEMS (starting in November 2020). We use $HCHO/NO_2$ and NH_3/NO_2 indicators from the satellite data to diagnose O_3 and $PM_{2.5}$ chemical regimes and their trends.

2. Air quality observing system for South Korea

We make use of air quality observations in Korea from surface sites, aircraft, and satellites. The National Institute of Environmental Research (NIER) operates the AirKorea surface network of 642 monitoring sites as of 2023 (https://www.airkorea.or.kr/eng, last access: 12 August 2024), providing hourly data on CO, SO_2, NO_2, O_3, PM_{10} (smaller than 10 μm diameter), and $PM_{2.5}$ concentrations. Monthly VOCs data (56 species) are available at a few urban sites. The KORUS-AQ field campaign in May−June 2016 included a detailed chemical payload onboard the DC-8 aircraft with extensive vertical profiling over the Seoul Metropolitan Area (SMA) at different times of day (Crawford et al., 2021). This was used by Yang et al. (2023) to infer diurnal profiles of NO_2 vertical column densities (VCDs) over the SMA and we will do the same here for HCHO and CHOCHO.

Satellite observations for air quality over Korea used in this work are compiled in Table 1 and are applied to analyze annual, diurnal, and spatial variations of pollutants. We filter out cloudy scenes using a cloud fraction threshold of 0.3 and apply additional quality filtering as recommended by the retrieval teams. GOCI and GOCI-II AOD retrievals are for 550 nm wavelength. CO is retrieved in both the shortwave and thermal infrared (SWIR and TIR). NH_3 is retrieved in the TIR. All other gases are retrieved in the ultraviolet-visible (UV-VIS). Tropospheric O_3 can also be retrieved in the UV but the measurements are difficult because of air scattering and the stratospheric column overhead, and different products are inconsistent over Korea (Gaudel et al., 2018). We do not use them here.

Table 1. Satellite observations used in this work.

Instrument	Launch	Species[a]	Spatial resolution[b]	Version	Reference
Low Earth orbit					
MOPITT	1999	CO	22×22 km^2	V9	Deeter et al. (2022)
OMI	2004	SO_2, NO_2, HCHO, CHOCHO	13×24 km^2	V3[c]	González Abad et al. (2015); Krotkov et al. (2017); C. Li et al. (2020); Kwon et al. (2024)

TROPOMI	2017	CO , NO_2, HCHO	5.5 × 3.5 km^2	V2.4.0	De Smedt et al. (2018); Landgraf et al. (2016); van Geffen et al. (2022)
IASI	2006	NH_3	12 × 12 km^2	V4	Clarisse et al. (2023)
Geostationary orbit					
GEMS	2020	SO_2, NO_2[d], HCHO, CHOCHO	3.5 × 7.7 km^2	V2.0.0	Ha et al. (2024); G. T. Lee et al. (2024); NIER (2020) ; Oak et al. (2024)
GOCI	2011	AOD	2 × 2 km^2	YAER[e] V2	M. Choi et al. (2018)
GOCI-II	2020	AOD[f]	2.5 × 2.5 km^2	YAER	S. Lee et al. (2023)

[a] Total atmospheric columns except for NO_2 (tropospheric column).
[b] Native pixel resolution of retrieval.
[c] Provided at 1° × 1° by Kwon et al. (2024).
[d] Bias-corrected by Oak et al. (2024).
[e] Yonsei Aerosol Retrieval.
[f] Observations within the range of GOCI AOD (−0.05 to 3.6) are used to account for the systematic low bias in GOCI-II compared to GOCI (S. Lee et al., 2023; Pendergrass et al., 2024).

3. Air quality distributions and trends in South Korea

Here we analyze spatial distributions and temporal trends of individual air pollutants using surface and satellite observations, and compare the trends to the annual bottom-up estimates of anthropogenic emissions from CAPSS, reported with a two-year lag (https://www.air.go.kr/eng/main.do, last access: 12 August 2024). CAPSS includes city/county/district (Korean; si/gun/gu) level emissions for source categories including fuel combustion, manufacturing, solvent use, mobile sources, agriculture, and anthropogenic biomass burning (biofuel, agriculture).

Figure 1 shows major anthropogenic source regions in Korea. There are seven major cities with populations larger than one million. The SMA (37–37.8° N, 126.4–127.5° E) is the largest urban area which includes Seoul, Incheon, and surrounding suburbs, with concentrated electronics and chemical industry. The southeast region including Busan and Ulsan is the second largest urban area and has petrochemical facilities, oil refineries, and steel/ship/automobile manufacturing industries.

3.1. Carbon monoxide (CO)

CO levels in Korea have consistently remained below the national air quality standards (9 ppmv 8-hour, 25 ppmv 1-hour) since the late 1990s (NIER, 2023). CO is nevertheless a useful tracer of pollution and plays an important role driving ozone formation in Korea (Gaubert et al., 2020; H. Kim et al., 2022). Anthropogenic CO emissions in CAPSS are 45% from transportation (passenger vehicles, heavy-duty vehicles, ships) and 32% from biomass burning (agricultural waste incineration, biofuels). Figures 2a–c compare 2021 CAPSS CO emissions with 2023 average surface CO and TROPOMI VCDs. Concentrations are highest in urban and industrial areas. Low VCDs along the east coast are due to topography. The effect of topography on VCDs is more apparent for CO than for other species because of the longer lifetime of CO and hence higher background (lower variability).

Figure 2d shows annual trends, demonstrating consistency between CAPSS and atmospheric observations. CAPSS emissions and AirKorea surface concentrations decrease at similar rates of -2.3 ± 1.7 and $-2.6 \pm 0.7\%\ a^{-1}$. MOPITT decreases at a rate of $-0.9 \pm 0.5\%\ a^{-1}$, slower than surface concentrations because of the background contribution to the VCD. Chong et al. (2023) previously found a MOPITT CO decrease of $-0.6 \pm 0.1\%\ a^{-1}$ during 2005–2018. It is estimated that Chinese emissions contributed 21–25% to the downward trend between 2016 and 2022 (J. Park et al., 2024; E. Kim et al., 2024). The 2019 spike found in both surface CO and VCDs is due to stagnant conditions (J. Cho et al., 2022). This also affected other pollutants as will be shown below.

3.2. Sulfur dioxide (SO_2)

SO_2 levels in Korea have consistently remained below the national air quality standards (20 ppbv annual, 50 ppbv 24-hour) over the past two decades due to large reductions of emissions from power plants and the petrochemical industry (NIER, 2023). There is continuing motivation for SO_2 emission controls to decrease $PM_{2.5}$ sulfate (SO_4^{2-}). Figures 3a–c compare 2021 CAPSS SO_2 emissions with 2023 average surface SO_2 and GEMS VCDs for all available observations.

GEMS displays enhancements in the SMA, mid-south coast (power plants, petrochemical/steel industry) and northeastern regions (cement/concrete/pulp industry), consistent with previously (2011–2016) identified OMI SO_2 hotspots (Chong et al., 2020).

Figure 3d shows good agreement between the CAPSS-reported emission trends and atmospheric observations. CAPSS-reported emissions have decreased at a rate of –9.9 ± 3.3% a^{-1}, while surface SO_2 concentrations and OMI VCDs have decreased at similar rates of –6% a^{-1} since 2015. Past trends (1999–2016) in Seoul showed that local emissions were the main drivers of the long-term decrease in surface SO_2 (J. Seo et al., 2018). J. Park et al. (2024) found that national mean surface SO_2 decreased by 41% from 2016 to 2022, owing to reductions in domestic (25%) and Chinese (16%) emissions.

3.3. Nitrogen dioxide (NO_2)

NO_2 levels exceeded the national standards (30 ppbv annual, 60 ppbv 24-hour) at 28% of the AirKorea sites in 2015 but fewer than 1% in 2022 (NIER, 2023). NO_x emissions in Korea are dominated by the transportation sector, accounting for 64% of the CAPSS inventory. Control of NO_x emissions is more recent than for CO and SO_2 and has been motivated not only by the NO_2 standards but also to reduce $PM_{2.5}$ NO_3^-. CAPSS NO_x emissions declined by 23% from 2015 to 2021 in response to policies including stronger regulation on heavy-duty diesel engines in 2016 (S. Song and G. Lee, 2020) and seasonal PM management plans implemented in 2019 (Bae et al., 2022; J. Jeong et al., 2024).

Figures 4a–c compare 2021 CAPSS NO_x emissions with 2023 average surface NO_2 and GEMS tropospheric VCDs. Here we use a GEMS product calibrated to TROPOMI to remove artifacts (Oak et al., 2024). Surface concentrations and VCDs display similar spatial distributions, with highest values in the SMA and other urban areas in the southeast. Figure 4d shows that surface NO_2 and OMI tropospheric VCDs have decreased over the 2015−2023 period by 32% and 36%, respectively. The trend in CAPSS-reported emissions (−4.8 ± 2.7% a^{-1}) is consistent with surface observations (−4.4 ± 0.8% a^{-1}) and OMI VCDs (−4.6 ± 0.8% a^{-1}) during 2015−2023. Meteorology-corrected trends in tropospheric VCDs observed by ground-based remote sensing instruments at urban sites decreased at similar rates (−5.0 to −5.4% a^{-1}) during 2015−2020 (Y. Choi et al., 2023). Long-term (2005−2019) records show that significant decreases in surface and OMI NO_2 began in 2015 (S. Seo et al., 2021). CAPSS shows in increase from 2015 to 2016, which is due to updates in emission factors (S. Choi et al., 2020). E. Kim et al. (2024) found that only 2% of the observed 23% decrease in surface NO_2 during 2016−2021 over Korea was attributable to the Chinese contribution.

Geostationary satellite observations provide additional information on diurnal variation. Figure 4e shows the 2021−2023 seasonal mean hourly variations of surface NO_2 and GEMS VCDs over the SMA. Both surface and column NO_2 are higher by a factor of two during the cold season, which can be explained by the longer NO_x lifetime (Shah et al., 2020). Surface NO_2 concentrations peak at 8−9 local time (LT) when daytime emissions accumulate in a shallow mixed layer, then decrease by dilution over the rest of the morning as the mixed layer grows from solar heating, returning to a secondary maximum in the evening when the mixed layer collapses (Moutinho et al., 2020). In contrast, VCDs increase steadily in the morning as they are not affected by mixed layer growth, reaching a steady state in the cold season as daytime emissions become balanced by ventilation, and an afternoon decrease in the warm season due to the additional effect of the daytime photochemical sink (Yang et al., 2024).

3.4. Nonmethane volatile organic compounds (NMVOCs)

NMVOCs emissions include important contributions from both anthropogenic and biogenic sources. More than half of anthropogenic VOCs (AVOCs) emissions in CAPSS are from solvent use while transportation is responsible for less than 10%, although the latter may be a severe underestimate (S. Song et al., 2019; Y. Kim and G. Lee, 2018; Kwon et al., 2021). CAPSS also does not account for residential emissions of volatile chemical products (VCPs), which could be large in Korea as indicated by observations of elevated ethanol during KORUS-AQ (Beaudry et al., 2024; Travis et al., 2024). Annual total AVOCs emissions are estimated to be a factor of two larger than biogenic VOCs (BVOCs) on a national level (Jang et al., 2020). However BVOCs play an important role in O_3 and SOA formation during summer (H. K. Kim et al., 2018; Oak et al., 2022; H. M. Lee and R. Park, 2022), when its emissions are comparable to those of AVOCs (J. Choi et al., 2022).

Figures 5a–b compare 2021 total AVOCs emissions from CAPSS and BVOCs emissions calculated from MEGAN (Model of Emissions of Gases and Aerosols from Nature) (Guenther et al., 2012). The two have contrasting distributions, with AVOCs mostly urban and industrial. Shown in Figure 5c is the distribution of BTEX (≡ benzene + toluene + ethylbenzene + xylenes) concentrations observed at AirKorea sites, with high values over urban areas consistent with CAPSS. Benzene is elevated on the west and southern coasts where it originates from the steel industry, oil refineries, and petrochemical facilities (Fried et al., 2020; C. Cho et al., 2021; Y. Seo et al., 2014). Toluene, xylenes, and ethylbenzene are abundant in the SMA (Y. Lee et al., 2023; S.-J. Kim et al., 2021; S. Song et al., 2019) due to emissions from traffic and solvent use (Simpson et al., 2020).

Figures 5d–e show spatial distributions of HCHO and CHOCHO VCDs from GEMS. These are common intermediates in the oxidation of NMVOCs, but CHOCHO is preferentially produced from aromatics (Kaiser et al., 2015; J. Li et al., 2016). Satellite observations are most sensitive to precursor NMVOCs with short lifetimes and prompt HCHO or CHOCHO yields including isoprene, alkenes, toluene, and xylenes (Palmer et al., 2003; Bates et al., 2021; Chan Miller et al., 2017). The GEMS CHOCHO and HCHO VCDs are elevated in major industrial regions, but CHOCHO shows hotspots for manufacturing industries while HCHO shows hotspots for petrochemical facilities. HCHO observations are also more distributed, reflecting the larger BVOCs contribution from isoprene.

Figure 5f shows the CHOCHO to HCHO ratio $R_{GF} = \mathrm{VCD_{CHOCHO}}/\mathrm{VCD_{HCHO}}$, illustrating the contrast in their sources. R_{GF} is generally higher under anthropogenic dominance (Chen et al., 2023). Values range from 0.02 in rural regions to more than 0.05 in the SMA and Busan. In the US, R_{GF} values are below 0.03 even under polluted conditions (Chan Miller et al., 2017) and are down to 0.01 in rural regions with dominant biogenic sources (Kaiser et al., 2015). GEMS R_{GF} values in Korea are higher everywhere, indicating a more important role for AVOCs emissions than in the US where these emissions have been strongly regulated for decades (Parrish et al., 2009; Warneke et al., 2012). Unlike for other pollutants and in contrast to the US, regulation of AVOCs emissions in Korea has been limited (S. Song and G. Lee, 2020; J. Kim et al., 2023). Figure 5g shows no significant trends in AVOCs emissions, surface BTEX, and satellite observations of CHOCHO and HCHO from OMI, TROPOMI and GEMS during 2015–2023.

Figure 6 compares diurnal variations of HCHO and CHOCHO VCDs in the SMA observed from GEMS and DC-8 aircraft profiles during KORUS-AQ (May−June 2016). Here we use airborne observations conducted below 8 km over the SMA. Mean loss frequencies of HCHO and CHOCHO against oxidation by OH and photolysis average 0.42 h^{-1} and 0.61 h^{-1}, respectively at 11−15 local time in these aircraft profiles. Computation of VCDs and loss frequencies from the KORUS-AQ data is described in the Supplement. We find that the GEMS columns are lower than the aircraft column and this has been previously reported as systematic low biases in satellite observations of CHOCHO and HCHO (Chan Miller et al., 2017; Zhu et al., 2016; Zhu et al., 2020). HCHO VCDs are more than twice higher during the warm season (April−September) than the cold season (October−March), consistent with a biogenic contribution to HCHO, while CHOCHO VCDs show no seasonal difference. GEMS and aircraft diurnal variations show HCHO and CHOCHO increases in the morning from photochemical production (G. T. Lee et al., 2024), flattening by midday. The aircraft data show a late afternoon rise in HCHO but that is not seen in the satellite data.

3.5. Ozone (O_3)

None of the AirKorea monitoring sites met the MDA8 standard of 60 ppbv for O_3 as of 2022 (NIER, 2023). O_3 peaks in May–June in Korea (Figure 7a) with contributions from domestic emissions, wildfires, stratospheric intrusions, and transport from China (H. M. Lee and R. Park, 2022). Several studies have reported on the O_3 increase in Korea over the past two decades, using different O_3 concentration metrics and time periods (J. Seo et al., 2018; Yeo and Kim, 2022; S. W. Kim et al., 2023). Our own analysis of the May–June 90th percentile MDA8 O_3 calculated for individual AirKorea sites and then averaged across all sites shows a rapid increase of 1.5 ± 0.4 ppbv a^{-1} for 2005–2014, and a slower rate of 0.8 ± 0.9 ppbv a^{-1} for 2015–2023 (Figure 7b).

Previous studies found that O_3 formation in major cities in Korea is in the VOC-sensitive regime, where decreasing NO_x emissions causes O_3 to increase (S. Kim et al., 2018; S. W. Kim et al., 2023; Oak et al., 2019; Souri et al., 2020; H. J. Lee et al., 2021). However, as NO_x emissions have decreased (Figure 4) whereas VOC emissions have not (Figure 5), O_3 formation may shift to a NO_x-sensitive regime. The HCHO to NO_2 column ratio (R_{FN} = VCD_{HCHO}/VCD_{NO2}), an indicator for O_3 sensitivity to NO_x versus VOCs (Duncan et al., 2010; Martin et al., 2004), increased steadily from 2015 to 2023 as seen from OMI, TROPOMI, and GEMS (Figure 7c). Based on the criteria from Duncan et al. (2010) the positive trend in R_{FN} implies that Korea is now mostly in the NO_x-sensitive regime ($R_{FN} > 2$). Figures 7d–e show May−June 2023 MDA8 O_3 and its sensitivity regimes inferred from GEMS R_{FN}. Most of the country is in a NO_x-sensitive regime while VOC-sensitive conditions are largely limited to the central SMA. The broader SMA and urban southeastern Korea are in a transition regime where O_3 is sensitive to both NO_x and VOCs emissions. These latter regions experience the most severe O_3 pollution as both NO_x and VOCs contribute to O_3 formation.

Also shown in Figure 7b are May−June MDA8 O_3 trends for AirKorea sites in different sensitivity regimes based on the 2023 GEMS R_{FN}. The O_3 increase during 2015−2023 is only found in the VOC-sensitive areas (1.6 ± 0.8 ppbv a^{-1}). O_3 in NO_x-sensitive areas does not show any noticeable increase. Reports of O_3 increases in Korea based on data from the AirKorea sites may be biased by the AirKorea sites being concentrated in the SMA, which has been mostly VOC-sensitive. But this is now changing as NO_x emissions decrease, and O_3 pollution in Korea is now poised to decrease everywhere in response to continued NO_x emission controls. In the US, national average O_3 levels started to level off in the 1990s and declined significantly afterwards, shifting from VOC- to NO_x-sensitive regimes in response to NO_x reduction (He et al., 2020). The 2023 US national average May−September 90^{th} percentile MDA8 O_3 is now slightly above 60 ppbv (US EPA, 2024). An additional challenge for Korea to meet its air quality standard is the high background originating from East Asia, estimated to be 55 ppbv in May−June (Colombi et al., 2023).

3.6. Particulate matter (PM)

PM levels have steadily decreased in Korea over the 2015–2023 period with more than 95% of the AirKorea sites meeting the annual PM_{10} standard (50 μg m^{-3}) since 2018. However, only 27% of sites met the $PM_{2.5}$ annual standard (15 μg m^{-3}) in 2022, and only 4% met the 24-hour standard (35 μg m^{-3}) (NIER, 2023). Figures 8a–c show that PM_{10}, $PM_{2.5}$, and GOCI AOD share similar spatial distributions. Annual trends in PM_{10} (−4.0 ± 1.7% a^{-1}), $PM_{2.5}$ (−5.0 ± 1.6% a^{-1}), and AOD (−5.5 ± 2.7% a^{-1}) over Korea during 2015−2023 are consistent (Figure 8d). J. Park et al. (2024) found that 14% of the observed 33% decrease in $PM_{2.5}$ during 2016−2022 over Korea was attributable to the Chinese contribution.

Figure 8e shows seasonal mean hourly variations of surface $PM_{2.5}$ and GOCI AOD. Surface $PM_{2.5}$ peaks in winter to early spring, mostly attributable to sulfate-nitrate-ammonium aerosols (Zhai et al., 2021) and is minimum in summer during the monsoon period (H. M. Lee et al., 2024). Conversely, AOD peaks in spring and summer (March−August) due to dust events, chemical production of secondary aerosols, and hygroscopic growth at high relative humidity

(Zhai et al., 2021). $PM_{2.5}$ peaks at 9−11 LT local time and then decreases until late afternoon as the mixed layer grows and dilutes surface concentrations (Jordan et al., 2020). AOD rises in the morning and peaks in midday reflecting photochemical production (Lennartson et al., 2018; P. Kim et al., 2015).

2015−2021 $PM_{2.5}$ observations in Seoul shows that all major $PM_{2.5}$ components decreased except for NO_3^-, which accounts for 25% of total $PM_{2.5}$ during winter to early spring (H. M. Lee et al., 2024). Winter NO_3^- formation depends non-linearly on NO_x and NH_3 emissions, with dominant sensitivity to either precursor that can be diagnosed from the NH_3/NO_2 VCD ratio and the NO_2 VCD in satellite observations (Dang et al., 2023; 2024). Figures 9a−b compare 2021 CAPSS NH_3 emissions and 2023 average NH_3 VCDs observed by IASI. 76% of anthropogenic NH_3 emissions in Korea originate from livestock manure management according to CAPSS. Transportation is also a significant source in urban areas (T. Park et al., 2023). Highest VCDs are found in the southern SMA, where livestock farming is concentrated, and corresponding to a $PM_{2.5}$ hotspot (Figure 8b). Despite high NH_3 emissions in the southeast coast, VCD enhancements are not observed there due to high SO_2 emissions (Figure 3a) and expected high SO_4^{2-} production converting gas-phase NH_3 to particle-phase ammonium (NH_4^+). Figure 9d indicates that annual total NH_3 emissions have shown little change while NH_3 VCDs have significantly increased since 2015. Decreases in SO_2 emissions and the resulting SO_4^{2-} in both Korea and China have left more NH_3 available for NO_3^- formation (J. Jeong et al., 2022).

Figure 9c shows NO_3^- sensitivity regimes inferred from GEMS NO_2 and IASI NH_3 VCDs during the cold season (October−March) in 2023, as diagnosed using the winter threshold from Dang et al. (2024). Figure 9e shows the evolution of the sensitivity regimes inferred from OMI NO_2 and IASI NH_3 from 2015 to 2023. As NO_x emissions have decreased, we find that NO_3^- formation over Korea has transited from an NH_3-sensitive to a NO_x-sensitive regime. NH_3-sensitive conditions are now largely limited to parts of the SMA, and as NO_x emissions continue to decrease we can expect NO_3^- formation to be controlled by NO_x emissions everywhere. Our analysis indicates that Korea will increasingly benefit from controlling NO_x emissions to improve both O_3 and $PM_{2.5}$ air quality in the future.

4. Conclusions

We analyzed the distributions and 2015–2023 trends of major air pollutants in South Korea using the AirKorea surface network and satellite observations. Air quality in Korea has improved for primary pollutants over the past two decades, but surface O_3 and $PM_{2.5}$ still widely exceed national standards despite emission controls.

Surface CO and SO_2 levels have stayed below air quality standards since the late 1990s, while NO_2 is now below the air quality standard at almost all AirKorea sites. Anthropogenic CO and SO_2 show steady and consistent declines from 2015 to 2023 in both surface concentrations and satellite vertical column densities (VCDs), consistent with the trends from the CAPSS national emissions inventory. NO_2 surface concentrations decreased by 32% from 2015 to 2023 while tropospheric NO_2 VCDs decreased by 36%, consistent with the 23% decrease of NO_x emissions in CAPSS.

Anthropogenic VOCs emissions, including a major contribution from aromatic compounds (BTEX), show no significant trend from 2015 to 2023 in the CAPSS inventory. This is consistent with BTEX observations at AirKorea sites and with HCHO and CHOCHO VCDs from satellites. Satellite HCHO observations show contributions from both anthropogenic and biogenic VOCs, while CHOCHO is more specifically associated with BTEX. Diurnal variations of HCHO and CHOCHO over the Seoul Metropolitan Area (SMA) observed from the GEMS geostationary satellite instrument show a morning increase and a leveling off by midday. Aircraft vertical columns over the SMA during the KORUS-AQ campaign show similar diurnal variations but a late afternoon HCHO increase.

Surface O_3 levels in Korea peak in May–June, and observations at AirKorea sites show an average increase of 0.8 ppbv a^{-1} in 90th percentile MDA8 O_3 from 2015 to 2023. Such an O_3 increase has been attributed to the effect of NO_x emission reductions under VOC-sensitive conditions for O_3 production. However, we find from the evolution of the satellite HCHO/NO_2 ratio from 2015 to 2023 that the O_3 formation regime in Korea has been shifting from VOC- to NO_x-sensitive. GEMS satellite observations for 2023 indicate that most regions in Korea are now NO_x-sensitive or in a transition regime, and that VOC-sensitive conditions are confined to the central SMA. We find that the O_3 increase at AirKorea sites is limited to sites still in the VOC-sensitive regime, whereas there is no O_3 increase for sites in the transition or NO_x-limited regimes. Our results suggest that O_3 across Korea is poised to decrease in response to continued NO_x emission controls.

Annual trends during 2015−2023 in PM_{10}, $PM_{2.5}$, and AOD show consistent decreases of 4−5% a^{-1}. Diurnal variations in AODs seen from the GOCI satellite instrument show the importance of photochemical production as a source of PM. The only $PM_{2.5}$ component not to show a significant decrease over the 2015−2023 period is nitrate (NO_3^-). From the NH_3/NO_2 ratio observed by satellites and its trend over the 2015−2023 period, we find that $PM_{2.5}$ NO_3^- formation in Korea was mostly NH_3-sensitive but has become increasingly NO_x-sensitive as NO_x emissions have decreased. As of 2023, NO_3^- formation across Korea is dominantly NO_x-sensitive except in parts of the SMA.

The vigorous NO_x emission controls in Korea starting in 2016 have not yet yielded results for decreasing O_3 and $PM_{2.5}$ NO_3^-. However, our results show that they have effectively shifted O_3 production from a VOC-sensitive to a NO_x-sensitive regime and NO_3^- formation from an NH_3-sensitive to a NO_x-sensitive regime. As NO_x emissions continue to decrease, the benefits for decreasing O_3 and $PM_{2.5}$ should become apparent.

Acknowledgement

This research has been supported by the Samsung Advanced Institute of Technology (grant no. A41602).

Data availability

AirKorea surface network data are available at https://www.airkorea.or.kr/eng. CAPSS annual emissions are available at https://www.air.go.kr/eng/main.do. KORUS-AQ aircraft data are available at https://www-air.larc.nasa.gov/cgi-bin/ArcView/korusaq. Satellite products are available at MOPITT CO https://l5ftl01.larc.nasa.gov:22000/misrl2l3/MOPITT/MOP03J.009/; OMI SO_2 https://dx.doi.org/10.5067/Aura/OMI/DATA3008, NO_2 https://dx.doi.org/10.5067/Aura/OMI/DATA3007, HCHO https://dx.doi.org/10.5067/Aura/OMI/DATA3010, CHOCHO https://doi.org/10.7910/DVN/Q1O2UE; TROPOMI CO https://dx.doi.org/10.5270/S5P-bj3nry0, NO_2 https://dx.doi.org/10.5270/S5P-9bnp8q8, HCHO https://dx.doi.org/10.5270/S5P-vg1i7t0; IASI NH_3 https://iasi.aeris-data.fr/nh3/; GEMS SO_2, HCHO, CHOCHO https://nesc.nier. go.kr/en/html/index.do, NO_2 https://doi.org/10.7910/DVN/ZQQJRO; GOCI AOD available upon request.

Author contributions

Original draft preparation, data processing, analysis, investigation, and visualization were done by YJO. DJJ contributed to project conceptualization. Review and editing were done by DJJ, DCP, RD, HC, SL, and JK. DCP, NKC, and SK provided additional resources and support in analysis.

Competing interests

The contact author has declared that none of the authors has any competing interests.

References

Bae, M., Kim, B.-U., Kim, H. C., Kim, J., and Kim, S.: Role of emissions and meteorology in the recent PM2.5 changes in China and South Korea from 2015 to 2018, Environmental Pollution, 270, 116233, https://doi.org/10.1016/j.envpol.2020.116233, 2021.

Bae, M., Kim, S., and Kim, S.: Quantitative Evaluation on the Drivers of PM2.5 Concentration Change in South Korea during the 1st - 3rd Seasonal PM2.5 Management Periods, Journal of Korean Society for Atmospheric Environment (Korean), 38, 610-623, 10.5572/KOSAE.2022.38.4.610, 2022.

Bates, K. H., Jacob, D. J., Li, K., Ivatt, P. D., Evans, M. J., Yan, Y., and Lin, J.: Development and evaluation of a new compact mechanism for aromatic oxidation in atmospheric models, Atmos. Chem. Phys., 21, 18351-18374, 10.5194/acp-21-18351-2021, 2021.

Beaudry, E., Jacob, D. J., Bates, K. H., Zhai, S., Yang, L. H., Pendergrass, D. C., Colombi, N. K., Simpson, I. J., Wisthaler, A., Hopkins, J. R., Li, K., and Liao, H.: Ethanol and methanol in South Korea and China: evidence for large emissions of volatile chemical products (VCPs), submitted to ACS ES&T Air, 2024.

Chan Miller, C., Jacob, D. J., Marais, E. A., Yu, K., Travis, K. R., Kim, P. S., Fisher, J. A., Zhu, L., Wolfe, G. M., Hanisco, T. F., Keutsch, F. N., Kaiser, J., Min, K. E., Brown, S. S., Washenfelder, R. A., González Abad, G., and Chance, K.: Glyoxal yield from isoprene oxidation and relation to formaldehyde: chemical mechanism, constraints from SENEX aircraft observations, and interpretation of OMI satellite data, Atmos. Chem. Phys., 17, 8725-8738, 10.5194/acp-17-8725-2017, 2017.

Chen, Y., Liu, C., Su, W., Hu, Q., Zhang, C., Liu, H., and Yin, H.: Identification of volatile organic compound emissions from anthropogenic and biogenic sources based on satellite observation of formaldehyde and glyoxal, Science of The Total Environment, 859, 159997, https://doi.org/10.1016/j.scitotenv.2022.159997, 2023.

Cho, C., Clair, J. M. S., Liao, J., Wolfe, G. M., Jeong, S., Kang, D. i., Choi, J., Shin, M.-H., Park, J., Park, J.-H., Fried, A., Weinheimer, A., Blake, D. R., Diskin, G. S., Ullmann, K., Hall, S. R., Brune, W. H., Hanisco, T. F., and Min, K.-E.: Evolution of formaldehyde (HCHO) in a plume originating from a petrochemical industry and its volatile organic compounds (VOCs) emission rate estimation, Elementa: Science of the Anthropocene, 9, 10.1525/elementa.2021.00015, 2021.

Cho, J.-H., Kim, H.-S., and Yoon, M.-B.: The influence of atmospheric blocking on regional PM10 aerosol transport to South Korea during February–March of 2019, Atmospheric Environment, 277, 119056, https://doi.org/10.1016/j.atmosenv.2022.119056, 2022.

Choi, J., Henze, D. K., Nawaz, M. O., and Malley, C. S.: Source Attribution of Health Burdens From Ambient PM2.5, O3, and NO2 Exposure for Assessment of South Korean National Emission Control Scenarios by 2050, GeoHealth, 8, e2024GH001042, https://doi.org/10.1029/2024GH001042, 2024.

Choi, J., Henze, D. K., Cao, H., Nowlan, C. R., González Abad, G., Kwon, H.-A., Lee, H.-M., Oak, Y. J., Park, R. J., Bates, K. H., Maasakkers, J. D., Wisthaler, A., and Weinheimer, A. J.: An Inversion Framework for Optimizing Non-Methane VOC Emissions Using Remote Sensing and Airborne Observations in Northeast Asia During the KORUS-AQ Field Campaign, Journal of Geophysical Research: Atmospheres, 127, e2021JD035844, https://doi.org/10.1029/2021JD035844, 2022.

Choi, M., Kim, J., Lee, J., Kim, M., Park, Y. J., Holben, B., Eck, T. F., Li, Z., and Song, C. H.: GOCI Yonsei aerosol retrieval version 2 products: an improved algorithm and error analysis with uncertainty estimation from 5-year validation over East Asia, Atmos. Meas. Tech., 11, 385-408, 10.5194/amt-11-385-2018, 2018.

Choi, S.-W., Kim, T., Lee, H.-K., Kim, H.-C., Han, J., Lee, K.-B., Lim, E.-h., Shin, S.-H., Jin, H.-A., Cho, E., Kim, Y.-M., and Yoo, C.: Analysis of the National Air Pollutant Emission Inventory (CAPSS 2016) and the Major Cause of Change in Republic of Korea, Asian Journal of Atmospheric Environment, 14, 422-445, 10.5572/ajae.2020.14.4.422, 2020.

Choi, S.-w., Cho, H., Hong, Y., Jo, H.-j., Park, M., Lee, H.-j., Choi, Y.-j., Shin, H.-h., Lee, D., Shin, E., Baek, W., Park, S.-k., Kim, E., Kim, H.-c., Song, S.-j., Park, Y., Kim, J., Baek, J., Kim, J., and Yoo, C.: Analysis of the National Air Pollutant Emissions Inventory (CAPSS 2018) Data and Assessment of Emissions Based on Air Quality Modeling in the Republic of Korea, Asian Journal of Atmospheric Environment, 16, 2022084, 10.5572/ajae.2022.084, 2022.

Choi, Y., Kanaya, Y., Takashima, H., Park, K., Lee, H., Chong, J., Kim, J. H., and Park, J.-S.: Changes in Tropospheric Nitrogen Dioxide Vertical Column Densities over Japan and Korea during the COVID-19 Using Pandora and MAX-DOAS, Aerosol and Air Quality Research, 23, 220145, 10.4209/aaqr.220145, 2023.

Chong, H., Lee, S., Cho, Y., Kim, J., Koo, J.-H., Pyo Kim, Y., Kim, Y., Woo, J.-H., and Hyun Ahn, D.: Assessment of air quality in North Korea from satellite observations, Environment International, 171, 107708, https://doi.org/10.1016/j.envint.2022.107708, 2023.

Chong, H., Lee, S., Kim, J., Jeong, U., Li, C., Krotkov, N., Nowlan, C., Al-Saadi, J., Janz, S., Kowalewski, M., Ahn, M.-H., Kang, M., Joanna, J., Haffner, D., Hu, L., Castellanos, P., Huey, L., Choi, M., Song, C., and Koo, J. H.: High-resolution mapping of SO2 using airborne observations from the GeoTASO instrument during the KORUS-AQ field study: PCA-based vertical column retrievals, Remote Sensing of Environment, 241, 111725, 10.1016/j.rse.2020.111725, 2020.

Clarisse, L., Franco, B., Van Damme, M., Di Gioacchino, T., Hadji-Lazaro, J., Whitburn, S., Noppen, L., Hurtmans, D., Clerbaux, C., and Coheur, P.: The IASI NH3 version 4 product: averaging kernels and improved consistency, Atmos. Meas. Tech., 16, 5009-5028, 10.5194/amt-16-5009-2023, 2023.

Colombi, N. K., Jacob, D. J., Yang, L. H., Zhai, S., Shah, V., Grange, S. K., Yantosca, R. M., Kim, S., and Liao, H.: Why is ozone in South Korea and the Seoul metropolitan area so high and increasing?, Atmos. Chem. Phys., 23, 4031-4044, 10.5194/acp-23-4031-2023, 2023.

Crawford, J. H., Ahn, J.-Y., Al-Saadi, J., Chang, L., Emmons, L. K., Kim, J., Lee, G., Park, J.-H., Park, R. J., Woo, J. H., Song, C.-K., Hong, J.-H., Hong, Y.-D., Lefer, B. L., Lee, M., Lee, T., Kim, S., Min, K.-E., Yum, S. S., Shin, H. J., Kim, Y.-W., Choi, J.-S., Park, J.-S., Szykman, J. J., Long, R. W., Jordan, C. E., Simpson, I. J., Fried, A., Dibb, J. E., Cho, S., and Kim, Y. P.: The Korea–United States Air Quality (KORUS-AQ) field study, Elementa: Science of the Anthropocene, 9, 10.1525/elementa.2020.00163, 2021.

Dang, R., Jacob, D. J., Zhai, S., Coheur, P., Clarisse, L., Van Damme, M., Pendergrass, D. C., Choi, J.-s., Park, J.-s., Liu, Z., and Liao, H.: Diagnosing the Sensitivity of Particulate Nitrate to Precursor Emissions Using Satellite Observations of Ammonia and Nitrogen Dioxide, Geophysical Research Letters, 50, e2023GL105761, https://doi.org/10.1029/2023GL105761, 2023.

Dang, R., Jacob, D. J., Zhai, S., Yang, L. H., Pendergrass, D. C., Coheur, P., Clarisse, L., Van Damme, M., Choi, J.-s., Park, J.-s., Liu, Z., Xie, P., and Liao, H.: A Satellite-Based Indicator for Diagnosing Particulate Nitrate Sensitivity to Precursor Emissions: Application to East Asia, Europe, and North America, Environmental Science & Technology, 10.1021/acs.est.4c08082, 2024.

Deeter, M., Francis, G., Gille, J., Mao, D., Martínez-Alonso, S., Worden, H., Ziskin, D., Drummond, J., Commane, R., Diskin, G., and McKain, K.: The MOPITT Version 9 CO product: sampling enhancements and validation, Atmos. Meas. Tech., 15, 2325-2344, 10.5194/amt-15-2325-2022, 2022.

De Smedt, I., Theys, N., Yu, H., Danckaert, T., Lerot, C., Compernolle, S., Van Roozendael, M., Richter, A., Hilboll, A., Peters, E., Pedergnana, M., Loyola, D., Beirle, S., Wagner, T., Eskes, H., van Geffen, J., Boersma, K. F., and Veefkind, P.: Algorithm theoretical baseline for formaldehyde retrievals from S5P TROPOMI and from the QA4ECV project, Atmos. Meas. Tech., 11, 2395-2426, 10.5194/amt-11-2395-2018, 2018.

Duncan, B. N., Yoshida, Y., Olson, J. R., Sillman, S., Martin, R. V., Lamsal, L., Hu, Y., Pickering, K. E., Retscher, C., Allen, D. J., and Crawford, J. H.: Application of OMI observations to a space-based indicator of NOx and VOC controls on surface ozone formation, Atmospheric Environment, 44, 2213-2223, https://doi.org/10.1016/j.atmosenv.2010.03.010, 2010.

Edwards, D. P., Emmons, L. K., Hauglustaine, D. A., Chu, D. A., Gille, J. C., Kaufman, Y. J., Pétron, G., Yurganov, L. N., Giglio, L., Deeter, M. N., Yudin, V., Ziskin, D. C., Warner, J., Lamarque, J.-F., Francis, G. L., Ho, S. P., Mao, D., Chen, J., Grechko, E. I., and Drummond, J. R.: Observations of carbon monoxide and aerosols from the Terra satellite: Northern Hemisphere variability, Journal of Geophysical Research: Atmospheres, 109, https://doi.org/10.1029/2004JD004727, 2004.

Fried, A., Walega, J., Weibring, P., Richter, D., Simpson, I. J., Blake, D. R., Blake, N. J., Meinardi, S., Barletta, B., Hughes, S. C., Crawford, J. H., Diskin, G., Barrick, J., Hair, J., Fenn, M., Wisthaler, A., Mikoviny, T., Woo, J.-H., Park, M., Kim, J., Min, K.-E., Jeong, S., Wennberg, P. O., Kim, M. J., Crounse, J. D., Teng, A. P., Bennett, R., Yang-Martin, M., Shook, M. A., Huey, G., Tanner, D., Knote, C., Kim, J., Park, R., and Brune, W.: Airborne formaldehyde and volatile organic compound measurements over the Daesan petrochemical complex on Korea's northwest coast during the Korea-United States Air

Quality study: Estimation of emission fluxes and effects on air quality, Elementa: Science of the Anthropocene, 8, 10.1525/elementa.2020.121, 2020.

Gaubert, B., Emmons, L. K., Raeder, K., Tilmes, S., Miyazaki, K., Arellano Jr, A. F., Elguindi, N., GraNIER, C., Tang, W., Barré, J., Worden, H. M., Buchholz, R. R., Edwards, D. P., Franke, P., Anderson, J. L., Saunois, M., Schroeder, J., Woo, J. H., Simpson, I. J., Blake, D. R., Meinardi, S., Wennberg, P. O., Crounse, J., Teng, A., Kim, M., Dickerson, R. R., He, H., Ren, X., Pusede, S. E., and Diskin, G. S.: Correcting model biases of CO in East Asia: impact on oxidant distributions during KORUS-AQ, Atmos. Chem. Phys., 20, 14617-14647, 10.5194/acp-20-14617-2020, 2020.

Gaudel, A., Cooper, O. R., Ancellet, G., Barret, B., Boynard, A., Burrows, J. P., Clerbaux, C., Coheur, P.-F., Cuesta, J., Cuevas, E., Doniki, S., Dufour, G., Ebojie, F., Foret, G., Garcia, O., Granados-Muñoz, M. J., Hannigan, J. W., Hase, F., Hassler, B., Huang, G., Hurtmans, D., Jaffe, D., Jones, N., Kalabokas, P., Kerridge, B., Kulawik, S., Latter, B., Leblanc, T., Le Flochmoën, E., Lin, W., Liu, J., Liu, X., Mahieu, E., McClure-Begley, A., Neu, J. L., Osman, M., Palm, M., Petetin, H., Petropavlovskikh, I., Querel, R., Rahpoe, N., Rozanov, A., Schultz, M. G., Schwab, J., Siddans, R., Smale, D., Steinbacher, M., Tanimoto, H., Tarasick, D. W., Thouret, V., Thompson, A. M., Trickl, T., Weatherhead, E., Wespes, C., Worden, H. M., Vigouroux, C., Xu, X., Zeng, G., and Ziemke, J.: Tropospheric Ozone Assessment Report: Present-day distribution and trends of tropospheric ozone relevant to climate and global atmospheric chemistry model evaluation, Elementa: Science of the Anthropocene, 6, 10.1525/elementa.291, 2018.

González Abad, G., Liu, X., Chance, K., Wang, H., Kurosu, T. P., and Suleiman, R.: Updated Smithsonian Astrophysical Observatory Ozone Monitoring Instrument (SAO OMI) formaldehyde retrieval, Atmos. Meas. Tech., 8, 19-32, 10.5194/amt-8-19-2015, 2015.

Guenther, A. B., Jiang, X., Heald, C. L., Sakulyanontvittaya, T., Duhl, T., Emmons, L. K., and Wang, X.: The Model of Emissions of Gases and Aerosols from Nature version 2.1 (MEGAN2.1): an extended and updated framework for modeling biogenic emissions, Geosci. Model Dev., 5, 1471-1492, 10.5194/gmd-5-1471-2012, 2012.

Ha, E. S., Park, R. J., Kwon, H. A., Lee, G. T., Lee, S. D., Shin, S., Lee, D. W., Hong, H., Lerot, C., De Smedt, I., Danckaert, T., Hendrick, F., and Irie, H.: First evaluation of the GEMS glyoxal products against TROPOMI and ground-based measurements, Atmos. Meas. Tech., 17, 6369-6384, 10.5194/amt-17-6369-2024, 2024.

He, H., Liang, X. Z., Sun, C., Tao, Z., and Tong, D. Q.: The long-term trend and production sensitivity change in the US ozone pollution from observations and model simulations, Atmos. Chem. Phys., 20, 3191-3208, 10.5194/acp-20-3191-2020, 2020.

Jang, Y., Eo, Y., Jang, M., Woo, J.-H., Kim, Y., Lee, J.-B., and Lim, J.-H.: Impact of Land Cover and Leaf Area Index on BVOC Emissions over the Korean Peninsula, Atmosphere, 11, 806, 2020.

Jeong, J. I., Seo, J., and Park, R. J.: Compromised Improvement of Poor Visibility Due to PM Chemical Composition Changes in South Korea, Remote Sensing, 14, 5310, 2022.

Jeong, J. I., Park, R. J., Song, C.-K., Yeh, S.-W., and Woo, J.-H.: Quantitative analysis of winter PM2.5 reduction in South Korea, 2019/20 to 2021/22: Contributions of meteorology and emissions, Science of The Total Environment, 907, 168179, https://doi.org/10.1016/j.scitotenv.2023.168179, 2024.

Jordan, C. E., Crawford, J. H., Beyersdorf, A. J., Eck, T. F., Halliday, H. S., Nault, B. A., Chang, L.-S., Park, J., Park, R., Lee, G., Kim, H., Ahn, J.-y., Cho, S., Shin, H. J., Lee, J. H., Jung, J., Kim, D.-S., Lee, M., Lee, T., Whitehill, A., Szykman, J., Schueneman, M. K., Campuzano-Jost, P., Jimenez, J. L., DiGangi, J. P., Diskin, G. S., Anderson, B. E., Moore, R. H., Ziemba, L. D., Fenn, M. A., Hair, J. W., Kuehn, R. E., Holz, R. E., Chen, G., Travis, K., Shook, M., Peterson, D. A., Lamb, K. D., and Schwarz, J. P.: Investigation of factors controlling PM2.5 variability across the South Korean Peninsula during KORUS-AQ, Elementa: Science of the Anthropocene, 8, 10.1525/elementa.424, 2020.

Kaiser, J., Wolfe, G. M., Min, K. E., Brown, S. S., Miller, C. C., Jacob, D. J., deGouw, J. A., Graus, M., Hanisco, T. F., Holloway, J., Peischl, J., Pollack, I. B., Ryerson, T. B., Warneke, C., Washenfelder, R. A., and Keutsch, F. N.: Reassessing the ratio of glyoxal to formaldehyde as an indicator of hydrocarbon precursor speciation, Atmos. Chem. Phys., 15, 7571-7583, 10.5194/acp-15-7571-2015, 2015.

Kim, E., Kim, H. C., Kim, B.-U., Woo, J.-H., Liu, Y., and Kim, S.: Development of surface observation-based two-step emissions adjustment and its application on CO, NOx, and SO2 emissions in China and South Korea, Science of The Total Environment, 907, 167818, https://doi.org/10.1016/j.scitotenv.2023.167818, 2024.

Kim, H., Park, R. J., Kim, S., Brune, W. H., Diskin, G. S., Fried, A., Hall, S. R., Weinheimer, A. J., Wennberg, P., Wisthaler, A., Blake, D. R., and Ullmann, K.: Observed versus simulated OH reactivity during KORUS-AQ campaign: Implications for emission inventory and chemical environment in East Asia, Elementa: Science of the Anthropocene, 10, 10.1525/elementa.2022.00030, 2022.

Kim, H.-K., Song, C.-K., Han, K. M., Eo, Y. D., Song, C. H., Park, R., Hong, S.-C., Kim, S.-K., and Woo, J.-H.: Impact of biogenic emissions on early summer ozone and fine particulate matter exposure in the Seoul Metropolitan Area of Korea, Air Quality, Atmosphere & Health, 11, 1021-1035, 10.1007/s11869-018-0602-4, 2018.

Kim, J., Park, J., Hu, H., Crippa, M., Guizzardi, D., Chatani, S., Kurokawa, J., Morikawa, T., Yeo, S., Jin, H., and Woo, J.-H.: Long-term historical trends in air pollutant emissions in South Korea (2000–2018), Asian Journal of Atmospheric Environment, 17, 12, 10.1007/s44273-023-00013-w, 2023.

Kim, J., Jeong, U., Ahn, M.-H., Kim, J. H., Park, R. J., Lee, H., Song, C. H., Choi, Y.-S., Lee, K.-H., Yoo, J.-M., Jeong, M.-J., Park, S. K., Lee, K.-M., Song, C.-K., Kim, S.-W., Kim, Y. J., Kim, S.-W., Kim, M., Go, S., Liu, X., Chance, K., Chan Miller, C., Al-Saadi, J., Veihelmann, B., Bhartia, P. K., Torres, O., Abad, G. G., Haffner, D. P., Ko, D. H., Lee, S. H., Woo, J.-H., Chong, H., Park, S. S., Nicks, D., Choi, W. J., Moon, K.-J., Cho, A., Yoon, J., Kim, S.-k., Hong, H., Lee, K., Lee, H., Lee, S., Choi, M., Veefkind, P., Levelt, P. F., Edwards, D. P., Kang, M., Eo, M., Bak, J., Baek, K., Kwon, H.-A., Yang, J., Park, J., Han, K. M., Kim, B.-R., Shin, H.-W., Choi, H., Lee, E., Chong, J., Cha, Y., Koo, J.-H., Irie, H., Hayashida, S., Kasai, Y., Kanaya, Y., Liu, C., Lin, J., Crawford, J. H., Carmichael, G. R., Newchurch, M. J., Lefer, B. L., Herman, J. R., Swap, R. J., Lau, A. K. H., Kurosu, T. P., Jaross, G., Ahlers, B., Dobber, M., McElroy, C. T., and Choi, Y.: New Era of Air Quality Monitoring from Space: Geostationary Environment Monitoring Spectrometer (GEMS), Bulletin of the American Meteorological Society, 101, E1-E22, https://doi.org/10.1175/BAMS-D-18-0013.1, 2020.

Kim, P. S., Jacob, D. J., Fisher, J. A., Travis, K., Yu, K., Zhu, L., Yantosca, R. M., Sulprizio, M. P., Jimenez, J. L., Campuzano-Jost, P., Froyd, K. D., Liao, J., Hair, J. W., Fenn, M. A., Butler, C. F., Wagner, N. L., Gordon, T. D., Welti, A., Wennberg, P. O., Crounse, J. D., St. Clair, J. M., Teng, A. P., Millet, D. B., Schwarz, J. P., Markovic, M. Z., and Perring,

A. E.: Sources, seasonality, and trends of southeast US aerosol: an integrated analysis of surface, aircraft, and satellite observations with the GEOS-Chem chemical transport model, Atmos. Chem. Phys., 15, 10411-10433, 10.5194/acp-15-10411-2015, 2015.

Kim, S., Jeong, D., Sanchez, D., Wang, M., Seco, R., Blake, D., Meinardi, S., Barletta, B., Hughes, S., Jung, J., Kim, D., Lee, G., Lee, M., Ahn, J., Lee, S.-D., Cho, G., Sung, M.-Y., Lee, Y.-H., and Park, R.: The Controlling Factors of Photochemical Ozone Production in Seoul, South Korea, Aerosol and Air Quality Research, 18, 2253-2261, 10.4209/aaqr.2017.11.0452, 2018.

Kim, S.-J., Lee, S.-J., Lee, H.-Y., Park, H.-J., Kim, C.-H., Lim, H.-J., Lee, S.-B., Kim, J. Y., Schlink, U., and Choi, S.-D.: Spatial-seasonal variations and source identification of volatile organic compounds using passive air samplers in the metropolitan city of Seoul, South Korea, Atmospheric Environment, 246, 118136, https://doi.org/10.1016/j.atmosenv.2020.118136, 2021.

Kim, S. W., Kim, K. M., Jeong, Y., Seo, S., Park, Y., and Kim, J.: Changes in surface ozone in South Korea on diurnal to decadal timescales for the period of 2001–2021, Atmos. Chem. Phys., 23, 12867-12886, 10.5194/acp-23-12867-2023, 2023.

Kim, Y. P. and Lee, G.: Trend of Air Quality in Seoul: Policy and Science, Aerosol and Air Quality Research, 18, 2141-2156, 10.4209/aaqr.2018.03.0081, 2018.

Krotkov, N. A., Lamsal, L. N., Celarier, E. A., Swartz, W. H., Marchenko, S. V., Bucsela, E. J., Chan, K. L., Wenig, M., and Zara, M.: The version 3 OMI NO2 standard product, Atmos. Meas. Tech., 10, 3133-3149, 10.5194/amt-10-3133-2017, 2017

Kwon, H.-A., González Abad, G., Chan Miller, C., Hall, K. R., Nowlan, C. R., O’Sullivan, E., Wang, H., Chong, H., Ayazpour, Z., Liu, X., and Chance, K.: Updated OMI Glyoxal Column Measurements Using Collection 4 Level 1B Radiances, Earth and Space Science, 11, e2024EA003705, https://doi.org/10.1029/2024EA003705, 2024.

Kwon, H.-A., Park, R. J., Oak, Y. J., Nowlan, C. R., Janz, S. J., Kowalewski, M. G., Fried, A., Walega, J., Bates, K. H., Choi, J., Blake, D. R., Wisthaler, A., and Woo, J.-H.: Top-down estimates of anthropogenic VOC emissions in South Korea using formaldehyde vertical column densities from aircraft during the KORUS-AQ campaign, Elementa: Science of the Anthropocene, 9, 10.1525/elementa.2021.00109, 2021.

Landgraf, J., aan de Brugh, J., Scheepmaker, R., Borsdorff, T., Hu, H., Houweling, S., Butz, A., Aben, I., and Hasekamp, O.: Carbon monoxide total column retrievals from TROPOMI shortwave infrared measurements, Atmos. Meas. Tech., 9, 4955-4975, 10.5194/amt-9-4955-2016, 2016.

Lee, G. T., Park, R. J., Kwon, H. A., Ha, E. S., Lee, S. D., Shin, S., Ahn, M. H., Kang, M., Choi, Y. S., Kim, G., Lee, D. W., Kim, D. R., Hong, H., Langerock, B., Vigouroux, C., Lerot, C., Hendrick, F., Pinardi, G., De Smedt, I., Van Roozendael, M., Wang, P., Chong, H., Cho, Y., and Kim, J.: First evaluation of the GEMS formaldehyde product against TROPOMI and ground-based column measurements during the in-orbit test period, Atmos. Chem. Phys., 24, 4733-4749, 10.5194/acp-24-4733-2024, 2024.

Lee, H.-J., Chang, L.-S., Jaffe, D. A., Bak, J., Liu, X., Abad, G. G., Jo, H.-Y., Jo, Y.-J., Lee, J.-B., and Kim, C.-H.: Ozone Continues to Increase in East Asia Despite Decreasing NO2: Causes and Abatements, Remote Sensing, 13, 2177, 2021.

Lee, H.-M. and Park, R. J.: Factors determining the seasonal variation of ozone air quality in South Korea: Regional background versus domestic emission contributions, Environmental Pollution, 308, 119645, https://doi.org/10.1016/j.envpol.2022.119645, 2022.

Lee, H.-M., Kim, N. K., Ahn, J., Park, S.-M., Lee, J. Y., and Kim, Y. P.: When and why PM2.5 is high in Seoul, South Korea: Interpreting long-term (2015–2021) ground observations using machine learning and a chemical transport model, Science of The Total Environment, 920, 170822, https://doi.org/10.1016/j.scitotenv.2024.170822, 2024.

Lee, S., Choi, M., Kim, J., Park, Y.-J., Choi, J.-K., Lim, H., Lee, J., Kim, M., and Cho, Y.: Retrieval of aerosol optical properties from GOCI-II observations: Continuation of long-term geostationary aerosol monitoring over East Asia, Science of The Total Environment, 903, 166504, https://doi.org/10.1016/j.scitotenv.2023.166504, 2023.

Lee, Y., Won, S. R., Shin, H. J., Kim, D. G., and Lee, J. Y.: Seasonal Characteristics of Volatile Organic Compounds in Seoul, Korea: Major Sources and Contribution to Secondary Organic Aerosol Formation, Aerosol and Air Quality Research, 23, 220429, 10.4209/aaqr.220429, 2023.

Lennartson, E. M., Wang, J., Gu, J., Castro Garcia, L., Ge, C., Gao, M., Choi, M., Saide, P. E., Carmichael, G. R., Kim, J., and Janz, S. J.: Diurnal variation of aerosol optical depth and PM2.5 in South Korea: a synthesis from AERONET, satellite (GOCI), KORUS-AQ observation, and the WRF-Chem model, Atmos. Chem. Phys., 18, 15125-15144, 10.5194/acp-18-15125-2018, 2018.

Levelt, P. F., Oord, G. H. J. v. d., Dobber, M. R., Malkki, A., Huib, V., Johan de, V., Stammes, P., Lundell, J. O. V., and Saari, H.: The ozone monitoring instrument, IEEE Transactions on Geoscience and Remote Sensing, 44, 1093-1101, 10.1109/TGRS.2006.872333, 2006.

Li, J., Mao, J., Min, K.-E., Washenfelder, R. A., Brown, S. S., Kaiser, J., Keutsch, F. N., Volkamer, R., Wolfe, G. M., Hanisco, T. F., Pollack, I. B., Ryerson, T. B., Graus, M., Gilman, J. B., Lerner, B. M., Warneke, C., de Gouw, J. A., Middlebrook, A. M., Liao, J., Welti, A., Henderson, B. H., McNeill, V. F., Hall, S. R., Ullmann, K., Donner, L. J., Paulot, F., and Horowitz, L. W.: Observational constraints on glyoxal production from isoprene oxidation and its contribution to organic aerosol over the Southeast United States, Journal of Geophysical Research: Atmospheres, 121, 9849-9861, https://doi.org/10.1002/2016JD025331, 2016.

Li, C., Krotkov, N. A., Leonard, P. J. T., Carn, S., Joiner, J., Spurr, R. J. D., and Vasilkov, A.: Version 2 Ozone Monitoring Instrument SO2 product (OMSO2 V2): new anthropogenic SO2 vertical column density dataset, Atmos. Meas. Tech., 13, 6175-6191, 10.5194/amt-13-6175-2020, 2020.

Li, K., Jacob, D. J., Liao, H., Qiu, Y., Shen, L., Zhai, S., Bates, K. H., Sulprizio, M. P., Song, S., Lu, X., Zhang, Q., Zheng, B., Zhang, Y., Zhang, J., Lee, H. C., and Kuk, S. K.: Ozone pollution in the North China Plain spreading into the late-winter haze season, Proceedings of the National Academy of Sciences, 118, e2015797118, doi:10.1073/pnas.2015797118, 2021.

Martin, R. V., Fiore, A. M., and Van Donkelaar, A.: Space-based diagnosis of surface ozone sensitivity to anthropogenic emissions, Geophysical Research Letters, 31, https://doi.org/10.1029/2004GL019416, 2004.

Moutinho, J. L., Liang, D., Golan, R., Sarnat, S. E., Weber, R., Sarnat, J. A., and Russell, A. G.: Near-road vehicle emissions air quality monitoring for exposure modeling, Atmospheric Environment, 224, 117318, https://doi.org/10.1016/j.atmosenv.2020.117318, 2020.

NIER: Geostationary Environment Monitoring Spectrometer (GEMS) Algorithm Theoretical Basis Document SO_2 Retrieval Algorithm, https://nesc.nier.go.kr/en/html/satellite/doc/doc.do, 2020.

NIER: 2022 Air Quality Annual Report (Korean), https://airkorea.or.kr/web/detailViewDown?pMENU_NO=125, 2023.

Oak, Y. J., Park, R. J., Lee, J.-T., and Byun, G.: Future air quality and premature mortality in Korea, Science of The Total Environment, 865, 161134, https://doi.org/10.1016/j.scitotenv.2022.161134, 2023.

Oak, Y. J., Jacob, D. J., Balasus, N., Yang, L. H., Chong, H., Park, J., Lee, H., Lee, G. T., Ha, E. S., Park, R. J., Kwon, H. A., and Kim, J.: A bias-corrected GEMS geostationary satellite product for nitrogen dioxide using machine learning to enforce consistency with the TROPOMI satellite instrument, EGUsphere, 2024, 1-19, 10.5194/egusphere-2024-393, 2024.

Oak, Y. J., Park, R. J., Schroeder, J. R., Crawford, J. H., Blake, D. R., Weinheimer, A. J., Woo, J.-H., Kim, S.-W., Yeo, H., Fried, A., Wisthaler, A., and Brune, W. H.: Evaluation of simulated O3 production efficiency during the KORUS-AQ campaign: Implications for anthropogenic NOx emissions in Korea, Elementa: Science of the Anthropocene, 7, 10.1525/elementa.394, 2019.

Oak, Y. J., Park, R. J., Jo, D. S., Hodzic, A., Jimenez, J. L., Campuzano-Jost, P., Nault, B. A., Kim, H., Kim, H., Ha, E. S., Song, C.-K., Yi, S.-M., Diskin, G. S., Weinheimer, A. J., Blake, D. R., Wisthaler, A., Shim, M., and Shin, Y.: Evaluation of Secondary Organic Aerosol (SOA) Simulations for Seoul, Korea, Journal of Advances in Modeling Earth Systems, 14, e2021MS002760, https://doi.org/10.1029/2021MS002760, 2022.

Palmer, P. I., Jacob, D. J., Fiore, A. M., Martin, R. V., Chance, K., and Kurosu, T. P.: Mapping isoprene emissions over North America using formaldehyde column observations from space, Journal of Geophysical Research: Atmospheres, 108, https://doi.org/10.1029/2002JD002153, 2003.

Park, D.-H., Kim, S.-W., Kim, M.-H., Yeo, H., Park, S. S., Nishizawa, T., Shimizu, A., and Kim, C.-H.: Impacts of local versus long-range transported aerosols on PM10 concentrations in Seoul, Korea: An estimate based on 11-year PM10 and lidar observations, Science of The Total Environment, 750, 141739, https://doi.org/10.1016/j.scitotenv.2020.141739, 2021.

Park, J. P., Kim, E. K., Kang, Y.-H. K., and Kim, S.: Assessment of Provincial Air Quality based on Air Quality Index during 2016~2022, Journal of Korean Society for Atmospheric Environment (Korean), 40, 225-241, 2024.

Park, R. J., Oak, Y. J., Emmons, L. K., Kim, C.-H., Pfister, G. G., Carmichael, G. R., Saide, P. E., Cho, S.-Y., Kim, S., Woo, J.-H., Crawford, J. H., Gaubert, B., Lee, H.-J., Park, S.-Y., Jo, Y.-J., Gao, M., Tang, B., Stanier, C. O., Shin, S. S., Park, H. Y., Bae, C., and Kim, E.: Multi-model intercomparisons of air quality simulations for the KORUS-AQ campaign, Elementa: Science of the Anthropocene, 9, 10.1525/elementa.2021.00139, 2021.

Park, T., Singh, R., Ban, J., Kim, K., Park, G., Kang, S., Choi, S., Song, J., Yu, D.-G., Bae, M.-S., Ahn, J., Jung, H.-J., Lim, Y.-J., Kim, H. W., Hwang, T. K., Choi, Y. J., Kim, S.-Y., Kim, H. S., Chang, Y. W., Shin, H. J., Lim, Y., Lee, J., Park, J., Choi, J., and Lee, T.: Seasonal and regional variations of atmospheric ammonia across the South Korean Peninsula, Asian Journal of Atmospheric Environment, 17, 6, 10.1007/s44273-023-00008-7, 2023.

Parrish, D. D., Kuster, W. C., Shao, M., Yokouchi, Y., Kondo, Y., Goldan, P. D., de Gouw, J. A., Koike, M., and Shirai, T.: Comparison of air pollutant emissions among mega-cities, Atmospheric Environment, 43, 6435-6441, https://doi.org/10.1016/j.atmosenv.2009.06.024, 2009.

Pendergrass, D. C., Zhai, S., Kim, J., Koo, J. H., Lee, S., Bae, M., Kim, S., Liao, H., and Jacob, D. J.: Continuous mapping of fine particulate matter (PM2.5) air quality in East Asia at daily 6 × 6 km2 resolution by application of a random forest algorithm to 2011–2019 GOCI geostationary satellite data, Atmos. Meas. Tech., 15, 1075-1091, 10.5194/amt-15-1075-2022, 2022.

Pendergrass, D. C., Jacob, D. J., Oak, Y. J., Lee, J., Kim, M., Kim, J., Lee, S., Zhai, S., Irie, H., and Liao, H.: A continuous 2011-2022 record of fine particulate matter (PM2.5) in East Asia at daily 2-km resolution from geostationary satellite observations: population exposure and long-term trends, Earth Syst. Sci. Data Discuss., 2024, 1-27, 10.5194/essd-2024-172, 2024.

Seo, J., Park, D. S. R., Kim, J. Y., Youn, D., Lim, Y. B., and Kim, Y.: Effects of meteorology and emissions on urban air quality: a quantitative statistical approach to long-term records (1999–2016) in Seoul, South Korea, Atmos. Chem. Phys., 18, 16121-16137, 10.5194/acp-18-16121-2018, 2018.

Seo, S., Kim, S.-W., Kim, K.-M., Lamsal, L. N., and Jin, H.: Reductions in NO2 concentrations in Seoul, South Korea detected from space and ground-based monitors prior to and during the COVID-19 pandemic, Environmental Research Communications, 3, 051005, 10.1088/2515-7620/abed92, 2021.

Seo, Y.-K., Suvarapu, L., and Baek, S.-O.: Characterization of Odorous Compounds (VOC and Carbonyl Compounds) in the Ambient Air of Yeosu and Gwangyang, Large Industrial Areas of South Korea, TheScientificWorldJournal, 2014, 824301, 10.1155/2014/824301, 2014.

Shah, V., Jacob, D. J., Li, K., Silvern, R. F., Zhai, S., Liu, M., Lin, J., and Zhang, Q.: Effect of changing NOx lifetime on the seasonality and long-term trends of satellite-observed tropospheric NO2 columns over China, Atmos. Chem. Phys., 20, 1483-1495, 10.5194/acp-20-1483-2020, 2020.

Simpson, I. J., Blake, D. R., Blake, N. J., Meinardi, S., Barletta, B., Hughes, S. C., Fleming, L. T., Crawford, J. H., Diskin, G. S., Emmons, L. K., Fried, A., Guo, H., Peterson, D. A., Wisthaler, A., Woo, J.-H., Barré, J., Gaubert, B., Kim, J., Kim, M. J., Kim, Y., Knote, C., Mikoviny, T., Pusede, S. E., Schroeder, J. R., Wang, Y., Wennberg, P. O., and Zeng, L.: Characterization, sources and reactivity of volatile organic compounds (VOCs) in Seoul and surrounding regions during KORUS-AQ, Elementa: Science of the Anthropocene, 8, 10.1525/elementa.434, 2020.

Song, C.-K. and Lee, G.: Regional and Urban Air Quality in East Asia: South Korea, in: Handbook of Air Quality and Climate Change, edited by: Akimoto, H., and Tanimoto, H., Springer Nature Singapore, Singapore, 1-27, 10.1007/978-981-15-2527-8_70-1, 2020.

Song, S.-K., Shon, Z.-H., Kang, Y.-H., Kim, K.-H., Han, S.-B., Kang, M., Bang, J.-H., and Oh, I.: Source apportionment of VOCs and their impact on air quality and health in the megacity of Seoul, Environ Pollut, 247, 763-774, 10.1016/j.envpol.2019.01.102, 2019.

Souri, A. H., Nowlan, C. R., Wolfe, G. M., Lamsal, L. N., Chan Miller, C. E., Abad, G. G., Janz, S. J., Fried, A., Blake, D. R., Weinheimer, A. J., Diskin, G. S., Liu, X., and Chance, K.:

Revisiting the effectiveness of HCHO/NO2 ratios for inferring ozone sensitivity to its precursors using high resolution airborne remote sensing observations in a high ozone episode during the KORUS-AQ campaign, Atmospheric Environment, 224, 117341, https://doi.org/10.1016/j.atmosenv.2020.117341, 2020.

Travis, K. R., Nault, B. A., Crawford, J. H., Bates, K. H., Blake, D. R., Cohen, R. C., Fried, A., Hall, S. R., Huey, L. G., Lee, Y. R., Meinardi, S., Min, K. E., Simpson, I. J., and Ullman, K.: Impact of improved representation of volatile organic compound emissions and production of NOx reservoirs on modeled urban ozone production, Atmos. Chem. Phys., 24, 9555-9572, 10.5194/acp-24-9555-2024, 2024.

US EPA: Trends in Ozone Adjusted for Weather Conditions, https://www.epa.gov/air-trends/trends-ozone-adjusted-weather-conditions, 2024.

Van Damme, M., Clarisse, L., Heald, C. L., Hurtmans, D., Ngadi, Y., Clerbaux, C., Dolman, A. J., Erisman, J. W., and Coheur, P. F.: Global distributions, time series and error characterization of atmospheric ammonia (NH₃) from IASI satellite observations, Atmos. Chem. Phys., 14, 2905-2922, 10.5194/acp-14-2905-2014, 2014.

van Geffen, J., Eskes, H., Compernolle, S., Pinardi, G., Verhoelst, T., Lambert, J. C., Sneep, M., ter Linden, M., Ludewig, A., Boersma, K. F., and Veefkind, J. P.: Sentinel-5P TROPOMI NO2 retrieval: impact of version v2.2 improvements and comparisons with OMI and ground-based data, Atmos. Meas. Tech., 15, 2037-2060, 10.5194/amt-15-2037-2022, 2022.

Veefkind, J. P., Aben, I., McMullan, K., Förster, H., de Vries, J., Otter, G., Claas, J., Eskes, H. J., de Haan, J. F., Kleipool, Q., van Weele, M., Hasekamp, O., Hoogeveen, R., Landgraf, J., Snel, R., Tol, P., Ingmann, P., Voors, R., Kruizinga, B., Vink, R., Visser, H., and Levelt, P. F.: TROPOMI on the ESA Sentinel-5 Precursor: A GMES mission for global observations of the atmospheric composition for climate, air quality and ozone layer applications, Remote Sensing of Environment, 120, 70-83, https://doi.org/10.1016/j.rse.2011.09.027, 2012.

Warneke, C., de Gouw, J. A., Holloway, J. S., Peischl, J., Ryerson, T. B., Atlas, E., Blake, D., Trainer, M., and Parrish, D. D.: Multiyear trends in volatile organic compounds in Los Angeles, California: Five decades of decreasing emissions, Journal of Geophysical Research: Atmospheres, 117, https://doi.org/10.1029/2012JD017899, 2012.

Yang, L. H., Jacob, D. J., Colombi, N. K., Zhai, S., Bates, K. H., Shah, V., Beaudry, E., Yantosca, R. M., Lin, H., Brewer, J. F., Chong, H., Travis, K. R., Crawford, J. H., Lamsal, L. N., Koo, J. H., and Kim, J.: Tropospheric NO2 vertical profiles over South Korea and their relation to oxidant chemistry: implications for geostationary satellite retrievals and the observation of NO2 diurnal variation from space, Atmos. Chem. Phys., 23, 2465-2481, 10.5194/acp-23-2465-2023, 2023.

Yang, L. H., Jacob, D. J., Dang, R., Oak, Y. J., Lin, H., Kim, J., Zhai, S., Colombi, N. K., Pendergrass, D. C., Beaudry, E., Shah, V., Feng, X., Yantosca, R. M., Chong, H., Park, J., Lee, H., Lee, W. J., Kim, S., Kim, E., Travis, K. R., Crawford, J. H., and Liao, H.: Interpreting Geostationary Environment Monitoring Spectrometer (GEMS) geostationary satellite observations of the diurnal variation in nitrogen dioxide (NO2) over East Asia, Atmos. Chem. Phys., 24, 7027-7039, 10.5194/acp-24-7027-2024, 2024.

Yeo, M. J. and Kim, Y.: Long-term trends and affecting factors in the concentrations of criteria air pollutants in South Korea, Journal of Environmental Management, 317, 115458, 10.1016/j.jenvman.2022.115458, 2022.

Zhai, S., Jacob, D. J., Wang, X., Shen, L., Li, K., Zhang, Y., Gui, K., Zhao, T., and Liao, H.: Fine particulate matter (PM2.5) trends in China, 2013–2018: separating contributions from anthropogenic emissions and meteorology, Atmos. Chem. Phys., 19, 11031-11041, 10.5194/acp-19-11031-2019, 2019.

Zhai, S., Jacob, D. J., Brewer, J. F., Li, K., Moch, J. M., Kim, J., Lee, S., Lim, H., Lee, H. C., Kuk, S. K., Park, R. J., Jeong, J. I., Wang, X., Liu, P., Luo, G., Yu, F., Meng, J., Martin, R. V., Travis, K. R., Hair, J. W., Anderson, B. E., Dibb, J. E., Jimenez, J. L., Campuzano-Jost, P., Nault, B. A., Woo, J. H., Kim, Y., Zhang, Q., and Liao, H.: Relating geostationary satellite measurements of aerosol optical depth (AOD) over East Asia to fine particulate matter (PM2.5): insights from the KORUS-AQ aircraft campaign and GEOS-Chem model simulations, Atmos. Chem. Phys., 21, 16775-16791, 10.5194/acp-21-16775-2021, 2021.

Zhu, L., Jacob, D. J., Mickley, L. J., Marais, E. A., Cohan, D. S., Yoshida, Y., Duncan, B. N., González Abad, G., and Chance, K. V.: Anthropogenic emissions of highly reactive volatile organic compounds in eastern Texas inferred from oversampling of satellite (OMI) measurements of HCHO columns, Environmental Research Letters, 9, 114004, 10.1088/1748-9326/9/11/114004, 2014.

Zhu, L., Jacob, D. J., Kim, P. S., Fisher, J. A., Yu, K., Travis, K. R., Mickley, L. J., Yantosca, R. M., Sulprizio, M. P., De Smedt, I., González Abad, G., Chance, K., Li, C., Ferrare, R., Fried, A., Hair, J. W., Hanisco, T. F., Richter, D., Jo Scarino, A., Walega, J., Weibring, P., and Wolfe, G. M.: Observing atmospheric formaldehyde (HCHO) from space: validation and intercomparison of six retrievals from four satellites (OMI, GOME2A, GOME2B, OMPS) with SEAC4RS aircraft observations over the southeast US, Atmos. Chem. Phys., 16, 13477-13490, 10.5194/acp-16-13477-2016, 2016.

Zhu, L., González Abad, G., Nowlan, C. R., Chan Miller, C., Chance, K., Apel, E. C., DiGangi, J. P., Fried, A., Hanisco, T. F., Hornbrook, R. S., Hu, L., Kaiser, J., Keutsch, F. N., Permar, W., St. Clair, J. M., and Wolfe, G. M.: Validation of satellite formaldehyde (HCHO) retrievals using observations from 12 aircraft campaigns, Atmos. Chem. Phys., 20, 12329-12345, 10.5194/acp-20-12329-2020, 2020.

Figures

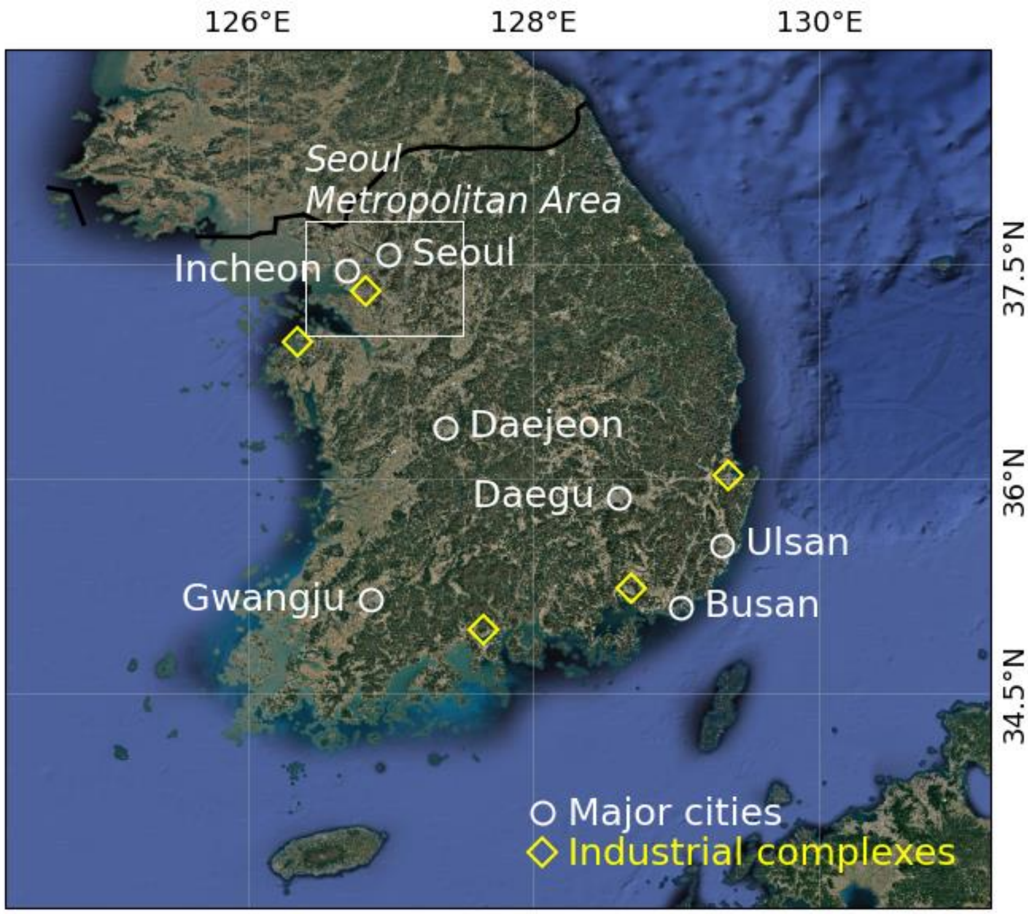

Figure 1. Geographic locations of major source regions in South Korea. Major cities and industrial complexes are indicated in white and yellow colors. The Seoul Metropolitan Area (SMA) is defined as the rectangular domain covering 37–37.8° N and 126.4–127.5° E. Background surface imagery is from © Google Earth.

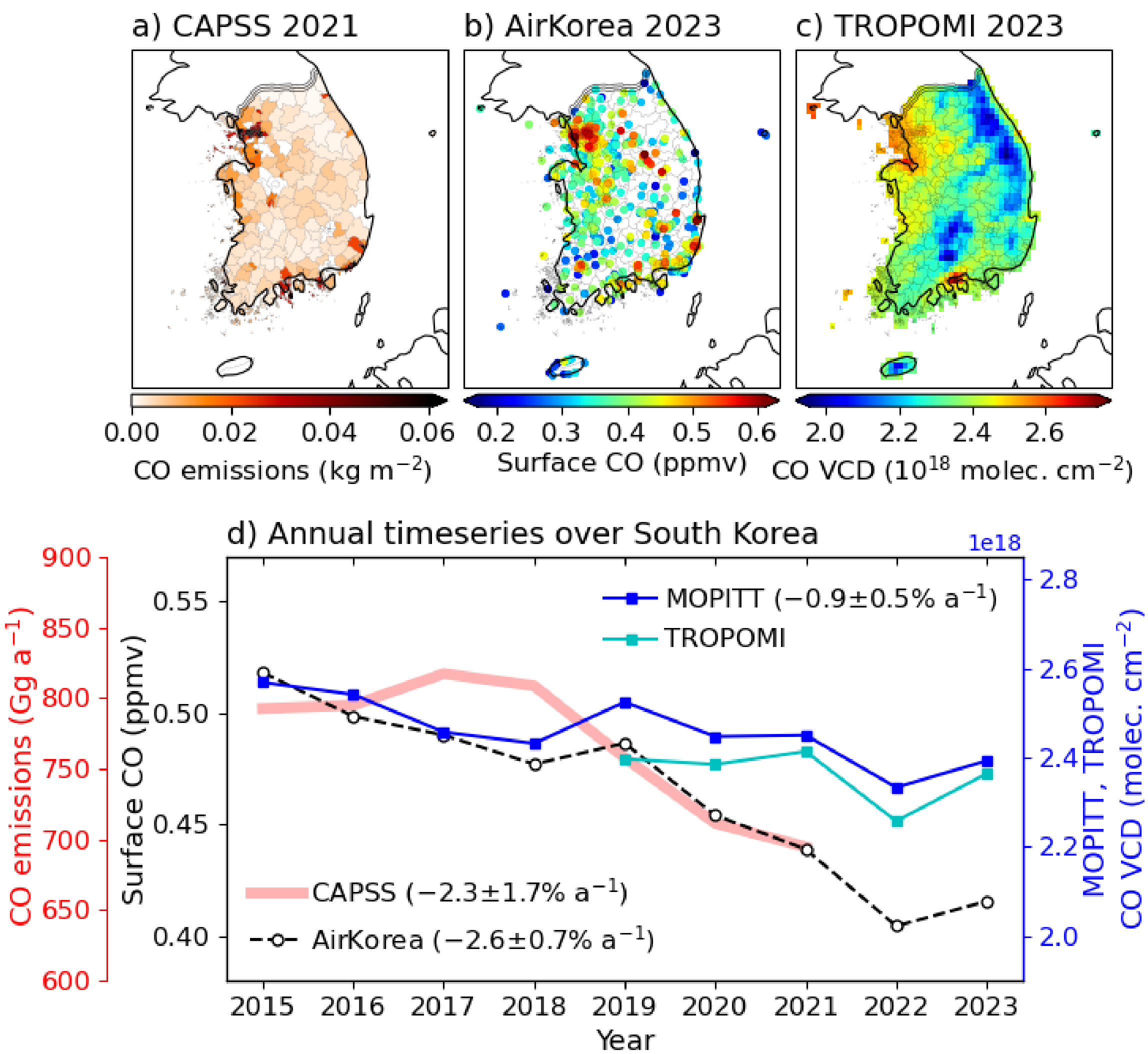

Figure 2. Annual mean CO distributions and trends in South Korea. Top panels show spatial distributions of (a) 2021 anthropogenic CO emissions from CAPSS, (b−c) 2023 average AirKorea surface CO concentrations and TROPOMI CO vertical column densities (VCDs). VCDs are mapped on a 0.1° × 0.1° grid. Lower panel (d) shows 2015−2023 trends in CAPSS CO emissions, surface CO averaged over all AirKorea sites, and CO VCDs from TROPOMI and MOPITT averaged over South Korea. Statistically significant trends (p-value < 0.05) are given inset.

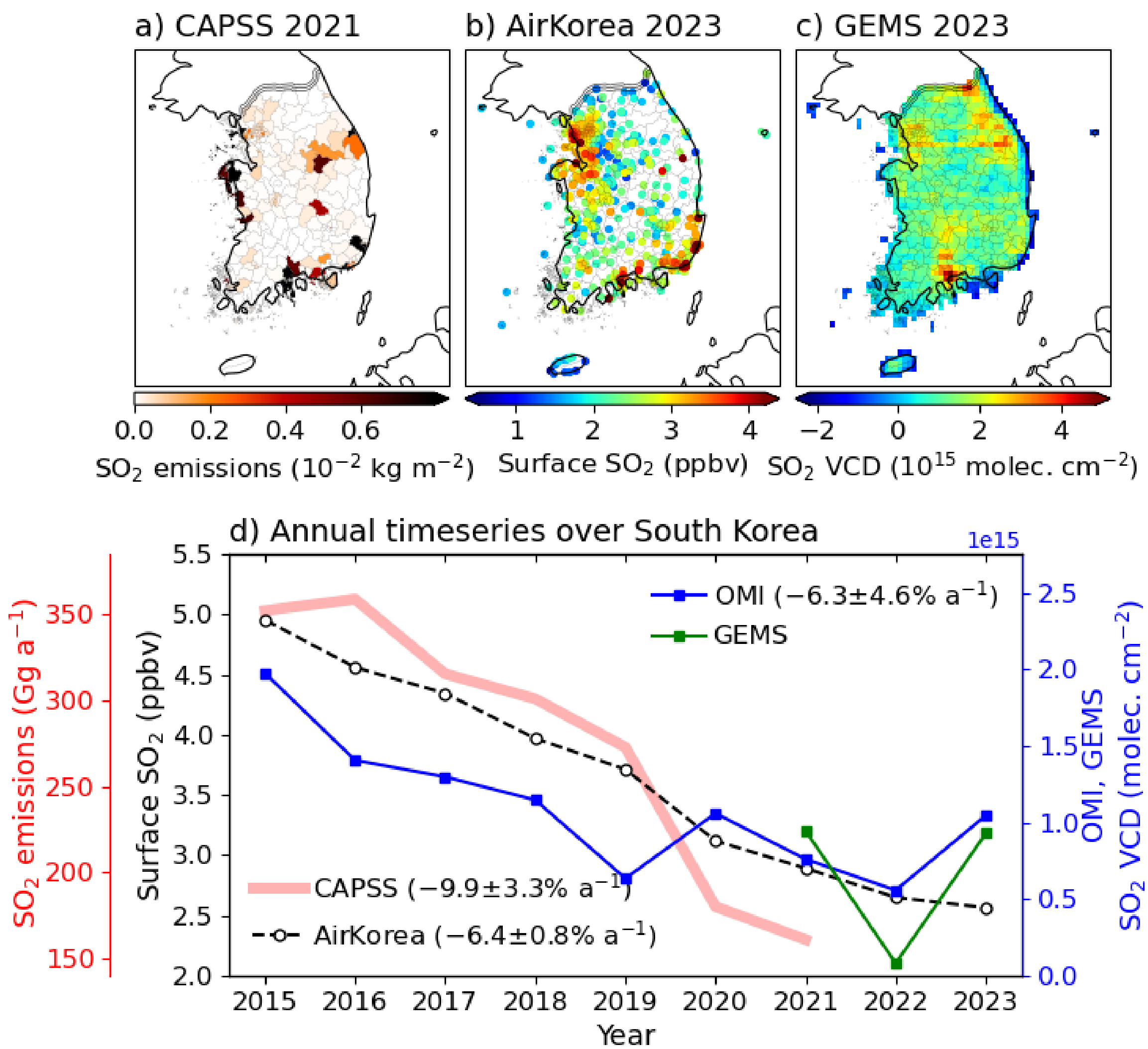

Figure 3. Annual mean SO_2 distributions and trends in South Korea. Top panels show spatial distributions of (a) 2021 anthropogenic SO_2 emissions from CAPSS, (b−c) 2023 average AirKorea surface SO_2 concentrations and GEMS SO_2 VCDs. VCDs are mapped on a 0.1° × 0.1° grid. Lower panel (d) shows 2015−2023 trends in CAPSS SO_2 emissions, surface SO_2 averaged over all AirKorea sites, and SO_2 VCDs from OMI and GEMS (sampled at OMI overpass time) averaged over South Korea. Statistically significant trends (p-value < 0.05) are given inset.

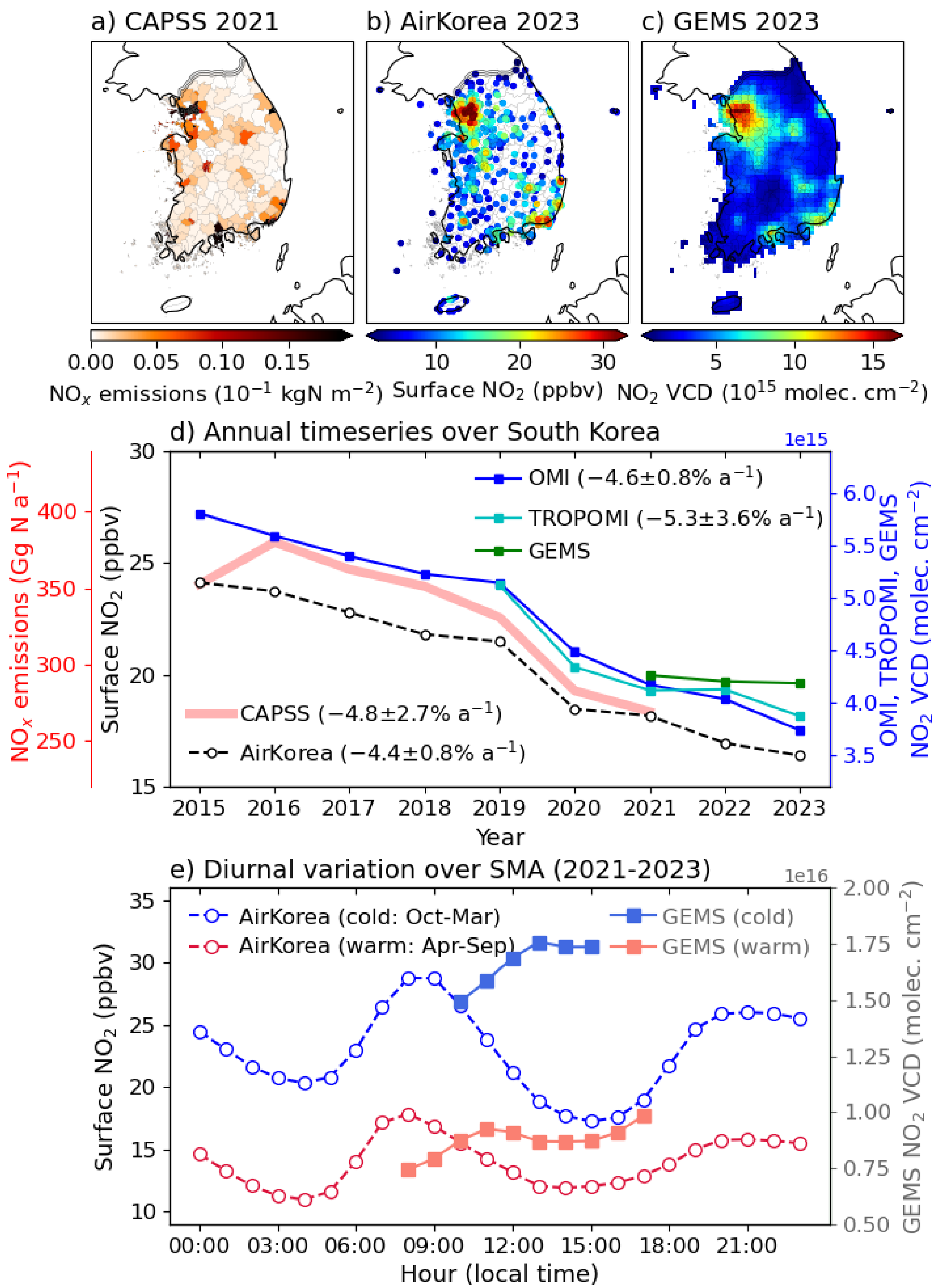

Figure 4. Annual mean NO_2 distributions and trends in South Korea. Top panels show spatial distributions of (a) 2021 anthropogenic NO_x emissions from CAPSS, (b−c) 2023 average AirKorea surface NO_2 concentrations and GEMS tropospheric NO_2 VCDs. VCDs are mapped on a 0.1° × 0.1° grid.

Middle panel (d) shows 2015−2023 trends in CAPSS NO_x emissions, surface NO_2 averaged over all AirKorea sites, and tropospheric NO_2 VCDs from OMI, TROPOMI, and GEMS (sampled at OMI overpass time) averaged over South Korea. Statistically significant trends (p-value < 0.05) are given inset. Lower panel (e) shows 2021−2023 seasonal mean (cold: October−March, warm: April−September) diurnal variations of AirKorea surface NO_2 concentrations and GEMS VCDs in the SMA.

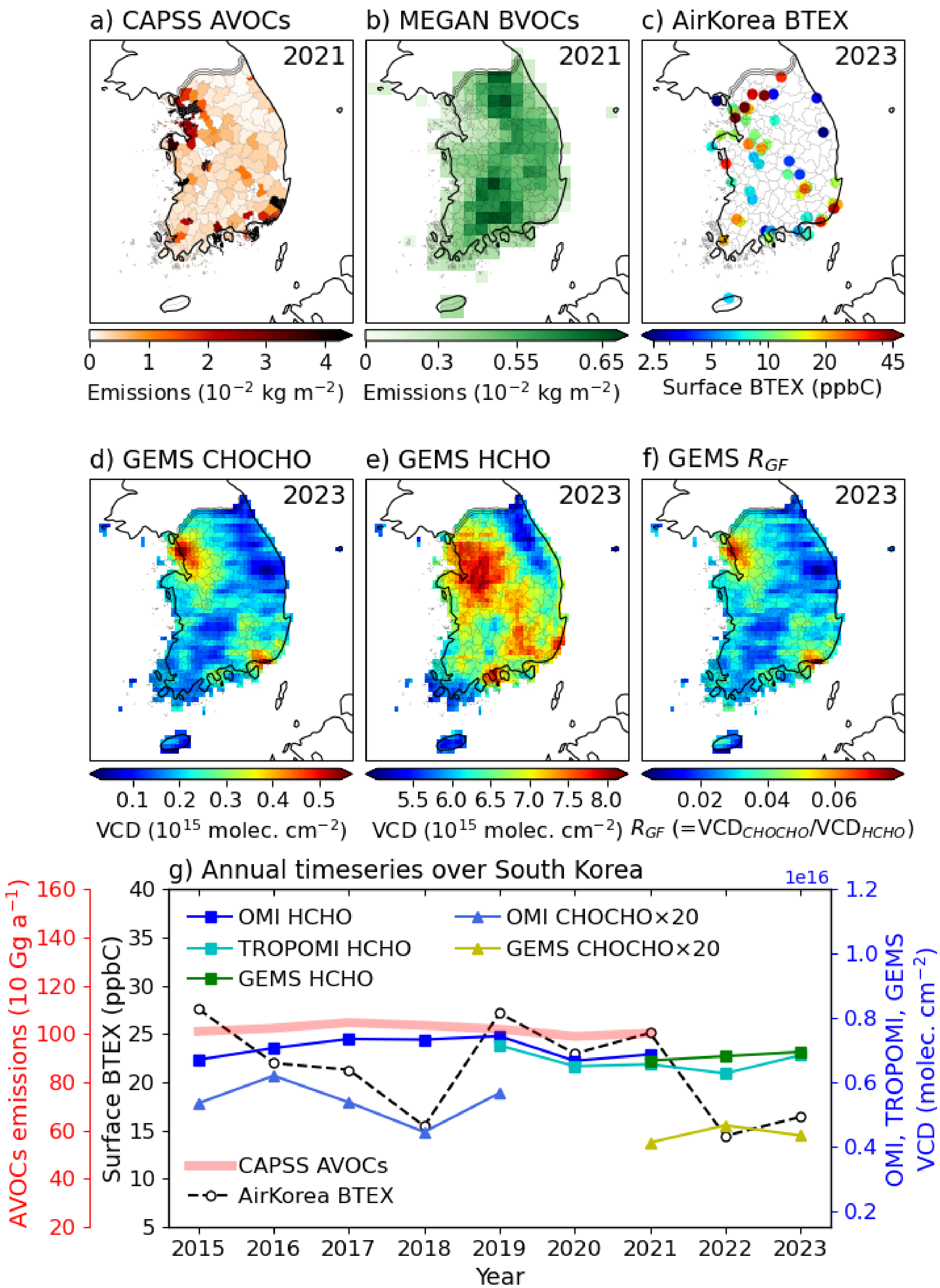

Figure 5. Annual mean NMVOC distributions and trends in South Korea. Top panels (a–b) show 2021 anthropogenic VOCs (AVOCs) emissions from CAPSS and biogenic VOCs (BVOCs: sum of isoprene, monoterpenes, sesquiterpenes, acetaldehyde, acetone, methanol, ethanol) emissions from MEGAN, and (c) 2023 average AirKorea surface BTEX (≡ benzene + toluene + ethylbenzene + xylenes)

concentrations. Middle panels (d−f) show spatial distributions of 2023 average GEMS glyoxal (CHOCHO) VCDs, formaldehyde (HCHO) VCDs, and glyoxal to formaldehyde ratio R_{GF} (= VCD_{CHOCHO}/VCD_{HCHO}) mapped on 0.1° × 0.1° grids. Lower panel (g) shows 2015−2023 trends in CAPSS AVOCs emissions, surface BTEX averaged over available AirKorea sites, and CHOCHO and HCHO VCDs from OMI, TROPOMI, and GEMS (sampled at OMI overpass time) averaged over South Korea. None of the data show significant trends over the 2015−2023 period.

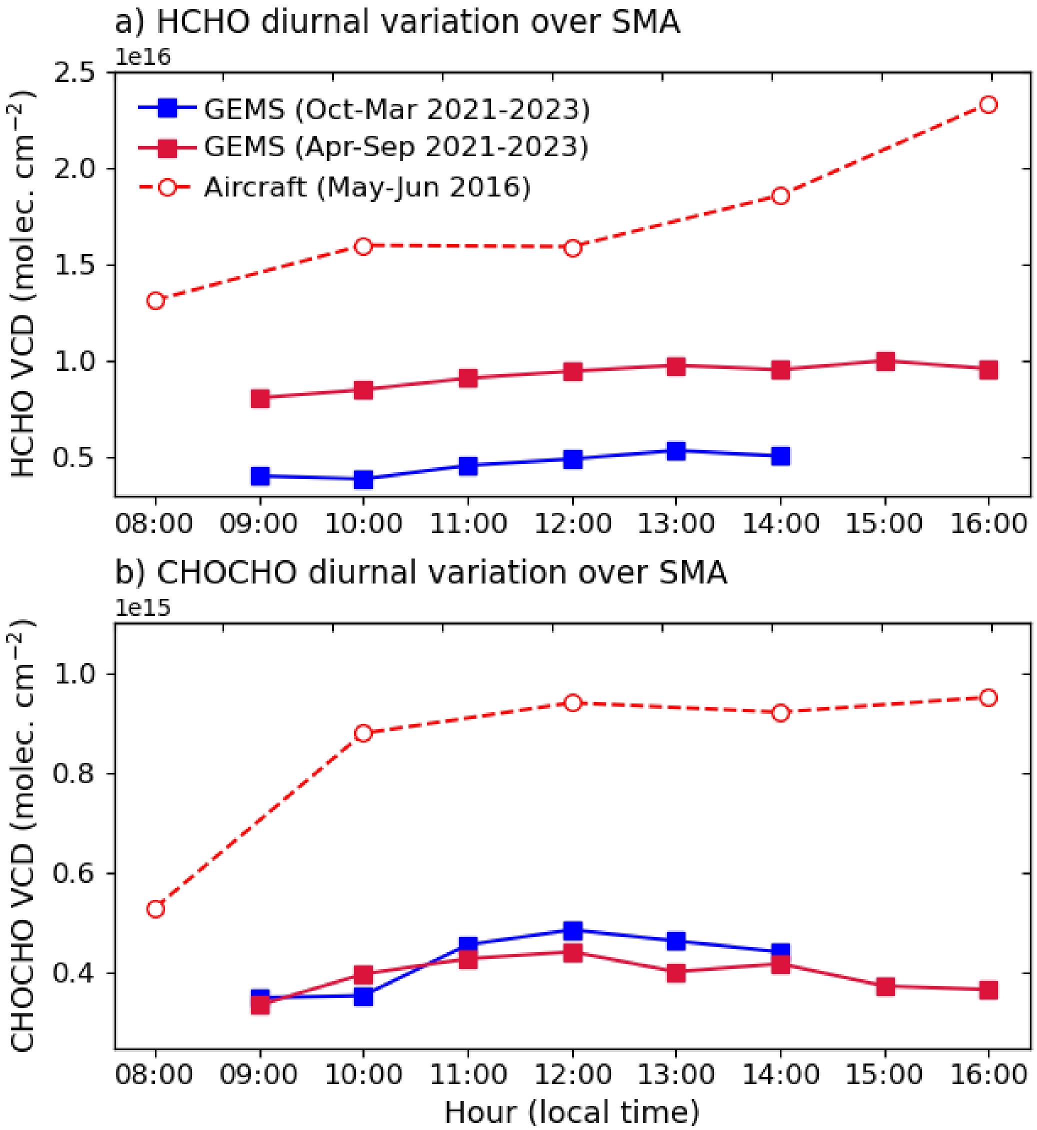

Figure 6. Diurnal variations of HCHO and CHOCHO VCDs in the SMA. Upper panel (a) shows seasonal mean (blue: October−March, red: April−September) diurnal variations of HCHO VCDs from GEMS 2021−2023 observations and KORUS-AQ (May−June 2016) DC-8 aircraft observations below 8 km altitude over the SMA. Lower panel (b) shows the same for CHOCHO VCDs.

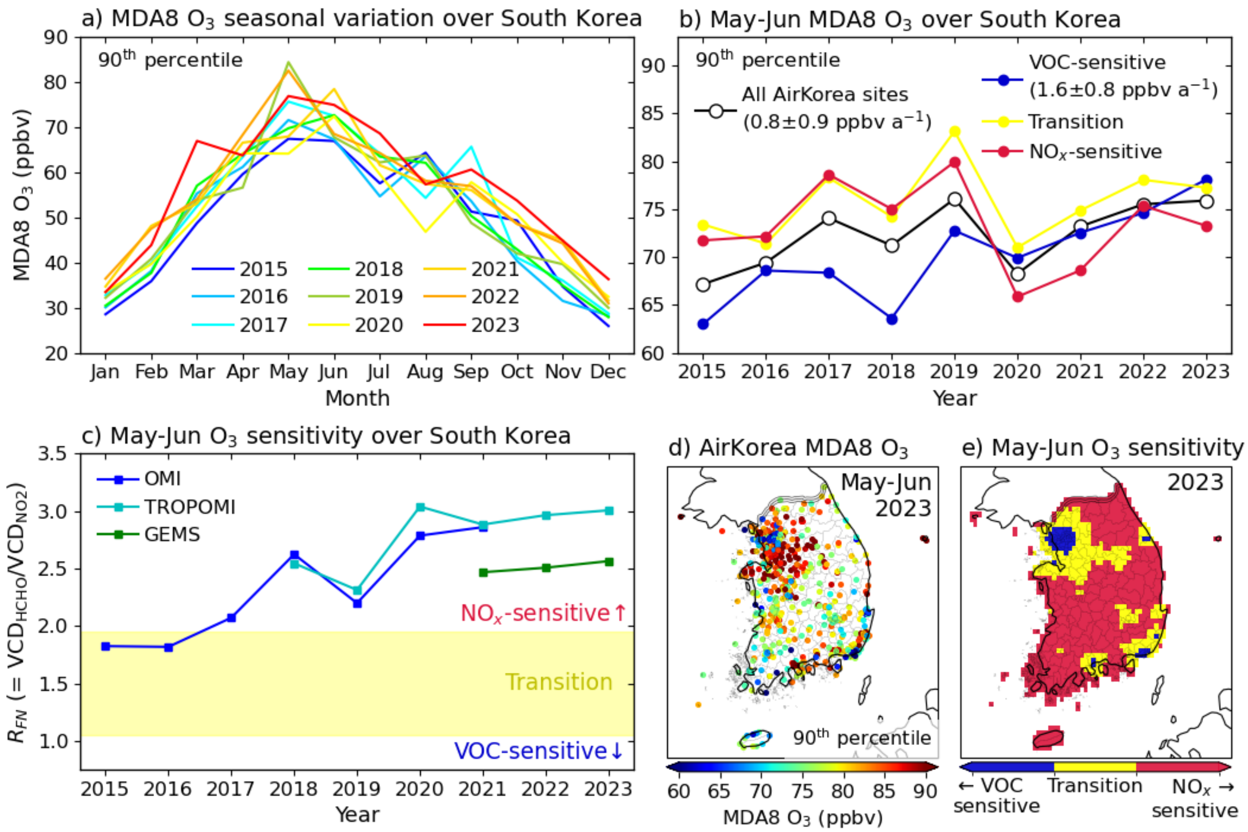

Figure 7. O_3 distribution, trend, and sensitivity to precursors in South Korea. Values are shown for the 90th percentile maximum 8-hour daily average (MDA8) at individual AirKorea sites. Top panels show averages of 90th percentile MDA8 O_3 for 2015−2023 as (a) monthly variations in individual years and (b) long-term trends in May−June (when concentrations are highest) for sites in different sensitivity regimes inferred from 2023 GEMS observations. Statistically significant trends (p-value < 0.05) are given inset. Lower left panel (c) shows May−June average timeseries of formaldehyde to NO_2 ratios R_{FN} (= VCD_{HCHO}/VCD_{NO2}) from OMI, TROPOMI, and GEMS (sampled at OMI overpass time). Lower right panels show spatial distributions of May−June 2023 average (d) AirKorea 90th percentile MDA8 O_3 and (e) O_3 sensitivity regimes inferred from GEMS R_{FN} mapped on a 0.1° × 0.1° grid. O_3 sensitivity regimes are based on R_{FN} thresholds from Duncan et al. (2010).

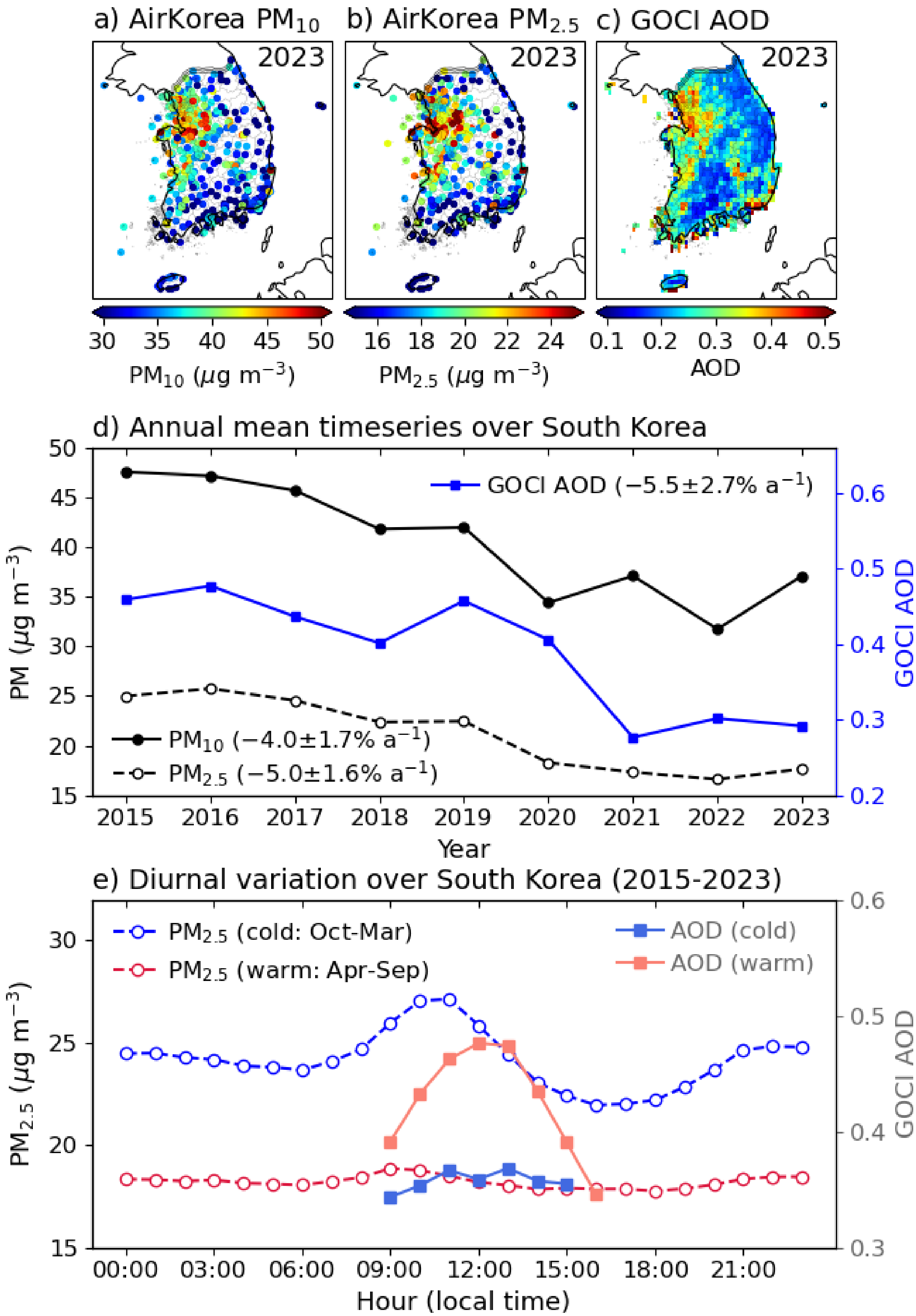

Figure 8. Annual mean PM and aerosol optical depth (AOD) distributions and trends in South Korea. Top panels (a−c) show spatial distributions of 2023 average AirKorea PM_{10} and $PM_{2.5}$, as well as

GOCI (GOCI; 2015–2020, GOCI-II; 2021–2023) AOD. AOD is mapped on a 0.1° × 0.1° grid. Middle panel (d) shows 2015−2023 trends in PM_{10} and $PM_{2.5}$ averaged over all AirKorea sites, and GOCI AOD averaged over South Korea. Statistically significant trends (p-value < 0.05) are given inset. Lower panel (e) shows 2015−2023 seasonal mean (cold: October−March, warm: April−September) diurnal variations of AirKorea $PM_{2.5}$ concentrations and GOCI AOD over South Korea.

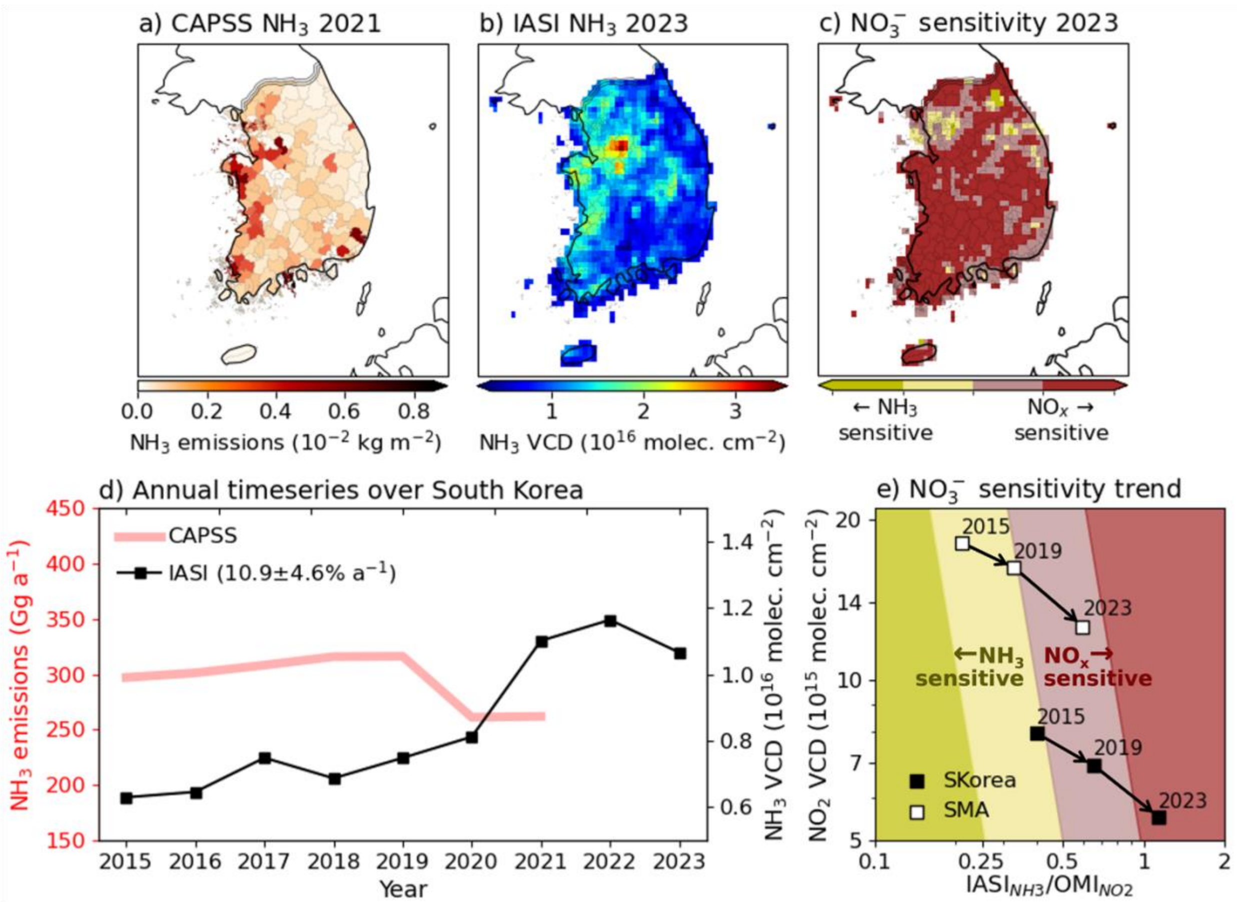

Figure 9. Annual mean NH_3 distributions, trends, and $PM_{2.5}$ nitrate (NO_3^-) sensitivity in South Korea. Top panels show spatial distributions of (a) 2021 anthropogenic NH_3 emissions from CAPSS, (b) 2023 average IASI NH_3 VCDs, and (c) 2023 cold season (October−March) NO_3^- sensitivity regimes inferred from IASI NH_3 and GEMS NO_2. VCDs are mapped on a 0.1° × 0.1° grid. Lower panel (d) shows 2015−2023 trends in CAPSS NH_3 emissions and IASI NH_3 VCDs averaged over South Korea. Statistically significant trends (p-value < 0.05) are given inset. Lower right panel (e) shows the cold season NO_3^- sensitivity trends averaged over South Korea and over the SMA. NO_3^- sensitivity regimes are based on winter thresholds from Dang et al. (2024).